Supplementary information

- Supplementary Figures 1-8

- Supplementary Note: Phase Field Model

- Supplementary Tables 1-7

Supplementary Figures 1-8

Figure S1

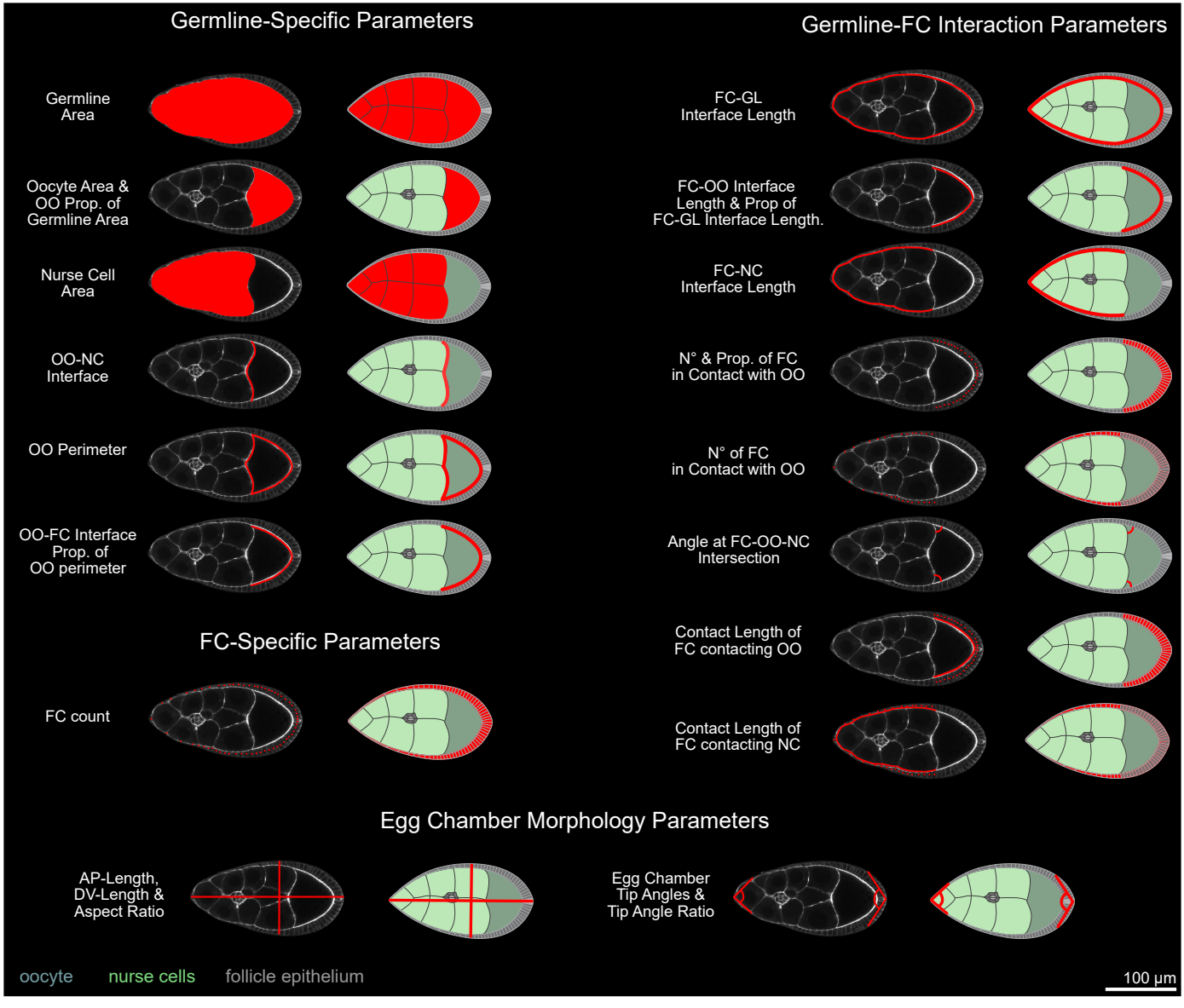
Germline-Specific Parameters
Germline Area
Oocyte Area & OO Prop. of Germline Area
Nurse Cell Area
OO-NC Interface
OO Perimeter
OO-FC Interface Prop. of OO perimeter
FC-Specific Parameters
FC count
Germline-FC Interaction Parameters
FC-GL Interface Length
FC-OO Interface Length & Prop of FC-GL Interface Length.
FC-NC Interface Length
N° & Prop. of FC in Contact with OO
N° of FC in Contact with OO
Angle at FC-OO-NC Intersection
Contact Length of FC contacting OO
Contact Length of FC contacting NC
Egg Chamber Morphology Parameters
AP-Length, DV-Length & Aspect Ratio
Egg Chamber Tip Angles & Tip Angle Ratio
oocyte
nurse cells
follicle epithelium
100 µm

Supplementary Figure 1

Drosophila egg chamber morphology parameters

Medial confocal sections and illustrations of phase 2 egg chambers visualizing parameters (red) that were quantified for the multidimensional morphology description.

Figure S2

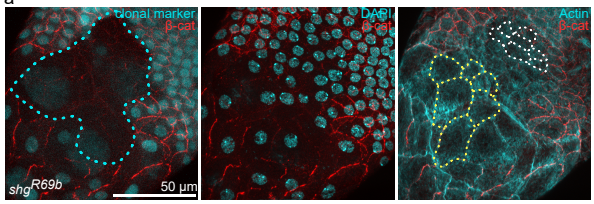
a
tional marker
β-cat
DAPI,
β-cat
Actin
β-cat
shgR69b
50 μm

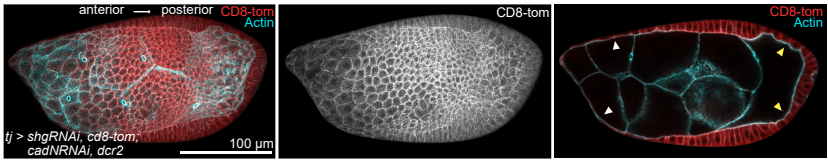
b
anterior → posterior
CD8-tom
Actin
CD8-tom
CD8-tom
Actin
tj > shgRNAi, cd8-tom;
cadNRNAi, dcr2
100 μm

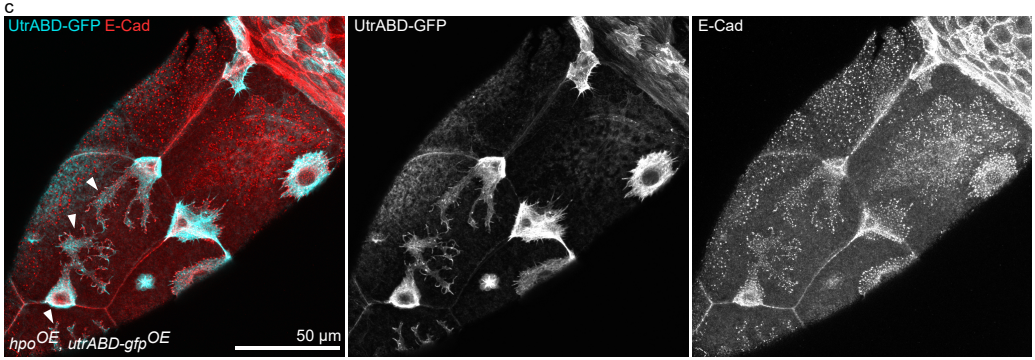
c
UtrABD-GFP E-Cad
UtrABD-GFP
E-Cad
hpoOE, utrABD-gfpOE
50 μm

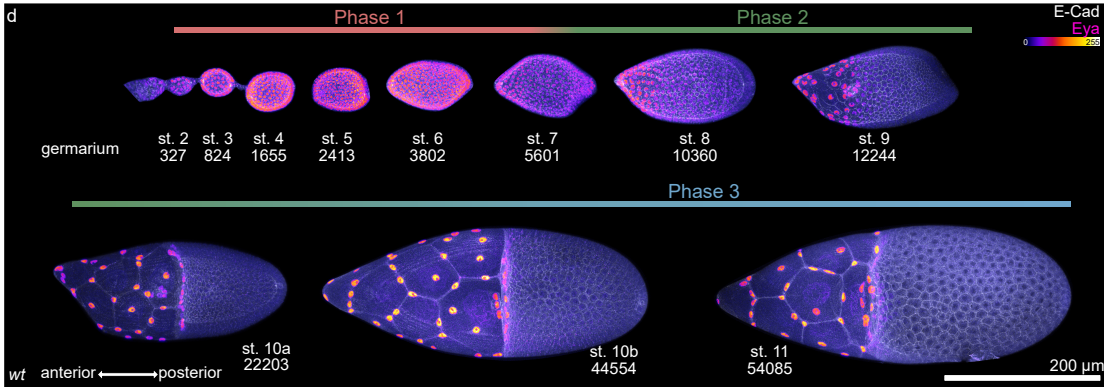
d
Phase 1
Phase 2
E-Cad
Eya
0
255
germarium
st. 2
327
st. 3
824
st. 4
1655
st. 5
2413
st. 6
3802
st. 7
5601
st. 8
10360
st. 9
12244
Phase 3
wt
anterior → posterior
st. 10a
22203
st. 10b
44554
st. 11
54085
200 μm

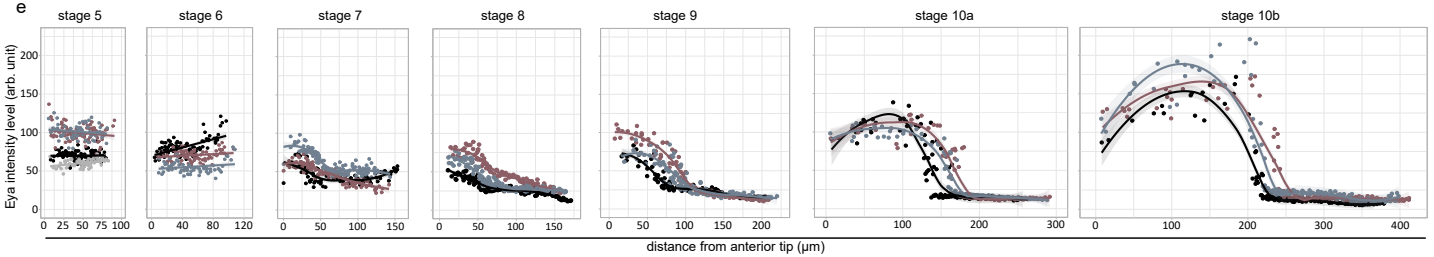
e
stage 5
stage 6
stage 7
stage 8
stage 9
stage 10a
stage 10b
Eya intensity level (arb. unit)
distance from anterior tip (μm)

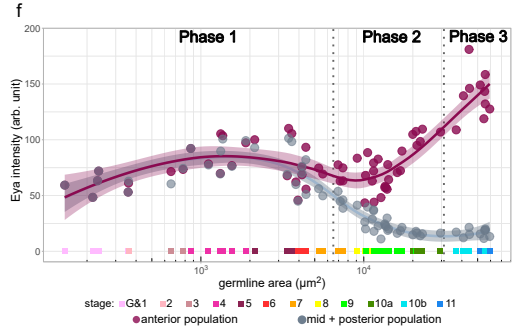
f
Phase 1
Phase 2
Phase 3
Eya intensity (arb. unit)
germline area (μm²)
stage: G&1 2 3 4 5 6 7 8 9 10a 10b 11
anterior population
mid + posterior population

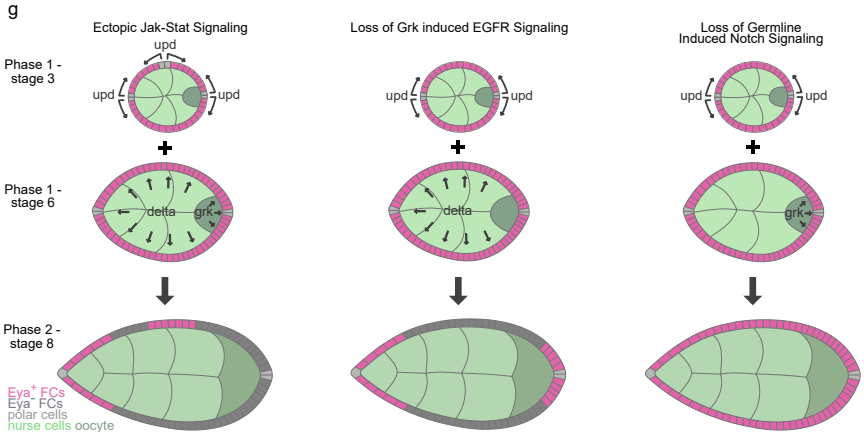
g
Ectopic Jak-Stat Signaling
Loss of Grk induced EGFR Signaling
Loss of Germline
Induced Notch Signaling
Phase 1 -
stage 3
upd
Phase 1 -
stage 6
delta
grk
Phase 2 -
stage 8
Eya+ FCs
Eya- FCs
polar cells
nurse cells oocyte

Supplementary Figure 2

AFCs spread actively over the nurse cell surface

a, Maximum fluorescence intensity projection of a *shg*^{R69b} (null mutant) clone (cyan dotted outline) in a phase 2 (stage 9) egg chamber consisting of AFCs and MBFCs. Stained for β-cat, F-Actin and nuclei (DAPI). Apical surfaces of AFCs (yellow) and MBFCs (white) are outlined. E-Cad loss does not disrupt AFC flattening, and MBFCs maintain their comparatively small apical areas.
b, Maximum fluorescence intensity projection of an egg chamber expressing s*hg-RNAi, cadN-RNAi, CD8-tom* and *dcr2* under the control of *tj-GAL4* (FC driver), stained for F-Actin. Loss of E-Cad and N-Cad causes disruption of PFC morphology (yellow arrowheads), but not of AFC spreading (white arrowheads).
c, Maximum fluorescence intensity projection of a phase 3 egg chamber with clonal overexpression of *hippo (hpo)* and *utrABD-gfp*, stained for E-Cad. *hpo* overexpression leads to reduced cell volume. AFCs detach from each other but continue to spread out cell autonomously (white arrowheads point at protrusions).
d, Maximum fluorescence intensity projections of representative egg chambers covering all three morphological phases, stained for E-Cad and Eya. Fire LUT visualizes Eya levels in nuclei of FCs throughout egg chamber development. Numbers denote germline area in µm^2.
e, Nuclear Eya levels in FCs as a function of their distance to the anterior pole of egg chambers from stages 5 to 10b. Colours represent individual egg chambers at each stage. Colours do not relate between stages. n (st. 5: 4 EC, st. 6-10b: 3 EC). Curves are LOESS fitted with a 95% CI area.
f, Measured mean Eya intensities in anterior (maroon) and mid+posterior (grey) FC populations of egg chambers as a function of germline area. Coloured squares represent developmental stages of egg chambers. Curves are LOESS fitted with a 95% CI area. (n=66 egg chambers). See Supp. File S2 for detailed stage-wise statistical comparison.
g, Illustrations of genetic manipulations targeting fate determining factors and the result on Eya expression in FCs of phase 2.
See Supplementary Table 7 for detailed statistical information. Source data are provided as a Source Data file.

Figure S3

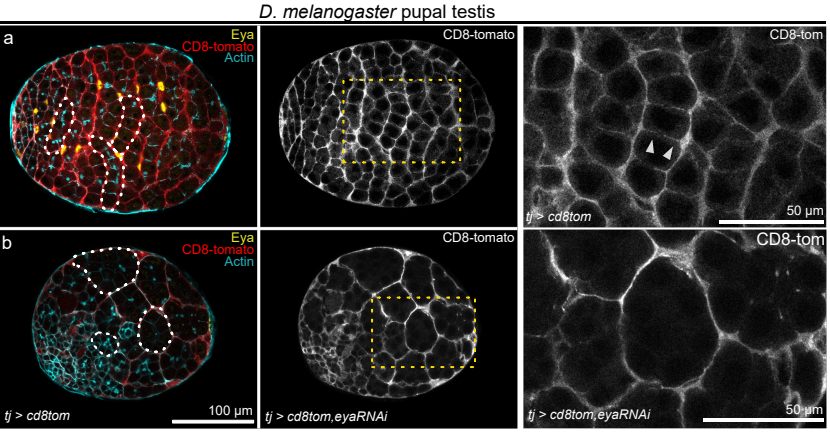
D. melanogaster pupal testis
a
Eya
CD8-tomato
Actin
CD8-tomato
CD8-tom
tj > cd8tom
50 µm
b
Eya
CD8-tomato
Actin
CD8-tomato
CD8-tom
tj > cd8tom
100 µm
tj > cd8tom,eyaRNAi
tj > cd8tom,eyaRNAi
50 µm

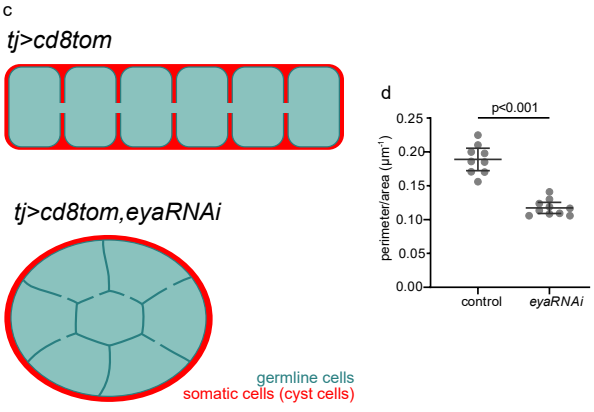
c
tj>cd8tom
tj>cd8tom,eyaRNAi
germline cells
somatic cells (cyst cells)
d
p<0.001
perimeter/area (µm⁻¹)
0.25
0.20
0.15
0.10
0.05
0.00
control
eyaRNAi

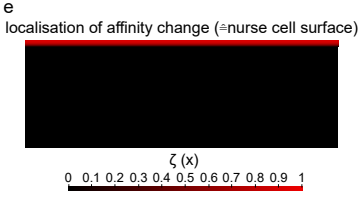
e
localisation of affinity change (≙nurse cell surface)
ζ (x)
0 0.1 0.2 0.3 0.4 0.5 0.6 0.7 0.8 0.9 1

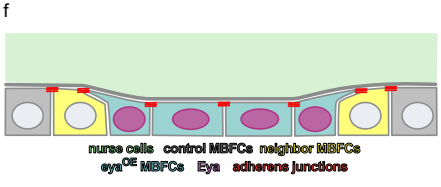
f
nurse cells
control MBFCs
neighbor MBFCs
eya OE MBFCs
Eya
adherens junctions

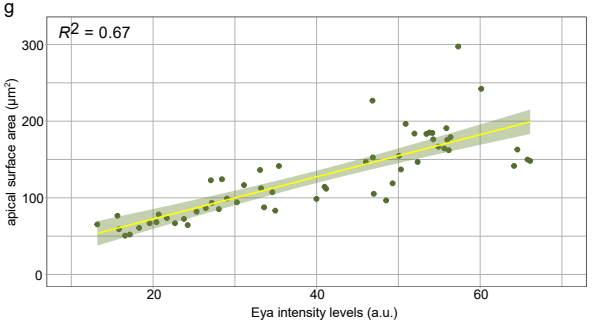
g
R^2 = 0.67
apical surface area (µm²)
300
200
100
0
20
40
60
Eya intensity levels (a.u.)

Supplementary Figure 3

Maximization of the soma-germline interface in testis depends on Eya

a, Confocal sections of *D. melanogaster* pupal testis expressing *CD8-tom* under the control of *tj-GAL4* (*tj>CD8tom*, cyst cell driver). *CD8-tom* visualizes somatic cells (cyst cells) that envelope the developing germline. Somatic cells extend between individual germline cells and thereby maximize the soma-germline contact surface (white arrowheads). White dotted lines mark individual germline cysts. Yellow dotted rectangular marks position of enlarged area.
b, Confocal sections of *D. melanogaster* pupal testis expressing *CD8-tom* and *eya-RNAi* under the control of *tj-GAL4* (*tj>CD8tom,eya-RNAi,* cyst cell driver). *CD8-tom* visualizes somatic cells (cyst cells) that envelope the developing germline. Note that loss of Eya causes failure of cyst cells extending between individual germline cells and that the germline cyst adopts a spherical shape. Consequently, the contact surface between somatic cells and germline cells is minimized. White dotted lines mark individual germline cysts. Yellow dotted rectangular marks position of enlarged area.
c, Illustrations of *tj>CD8-tom* and *tj>CD8-tom,eya-RNAi* spermatogonial cysts.
d, Quantification of the ratio between the germline cyst interface in contact with somatic cells and germline area. Mean+95%CI, two-tailed unpaired Student's t-test, n (*tj>CD8-tom*: 9 cysts, *tj>CD8-tom,eya-RNAi*: 10 cysts).
e, Localization of the affinity change that represents the nurse cell surface.
f, Illustration of cell morphologies upon ectopic eya^{OE} expression in MBFC clones in contact with nurse cells during phase 2. Corresponds to Fig. 3m.
g, Linear regression between apical surface areas and Eya levels of FCs (FC from anterior rows 1-7 of stage 9 egg chambers, phase 2). Linear regression with 95% CI area, n= 57 AFCs from 3 EC.
See Supplementary Table 7 for detailed statistical information. Source data are provided as a Source Data file.

Figure S4

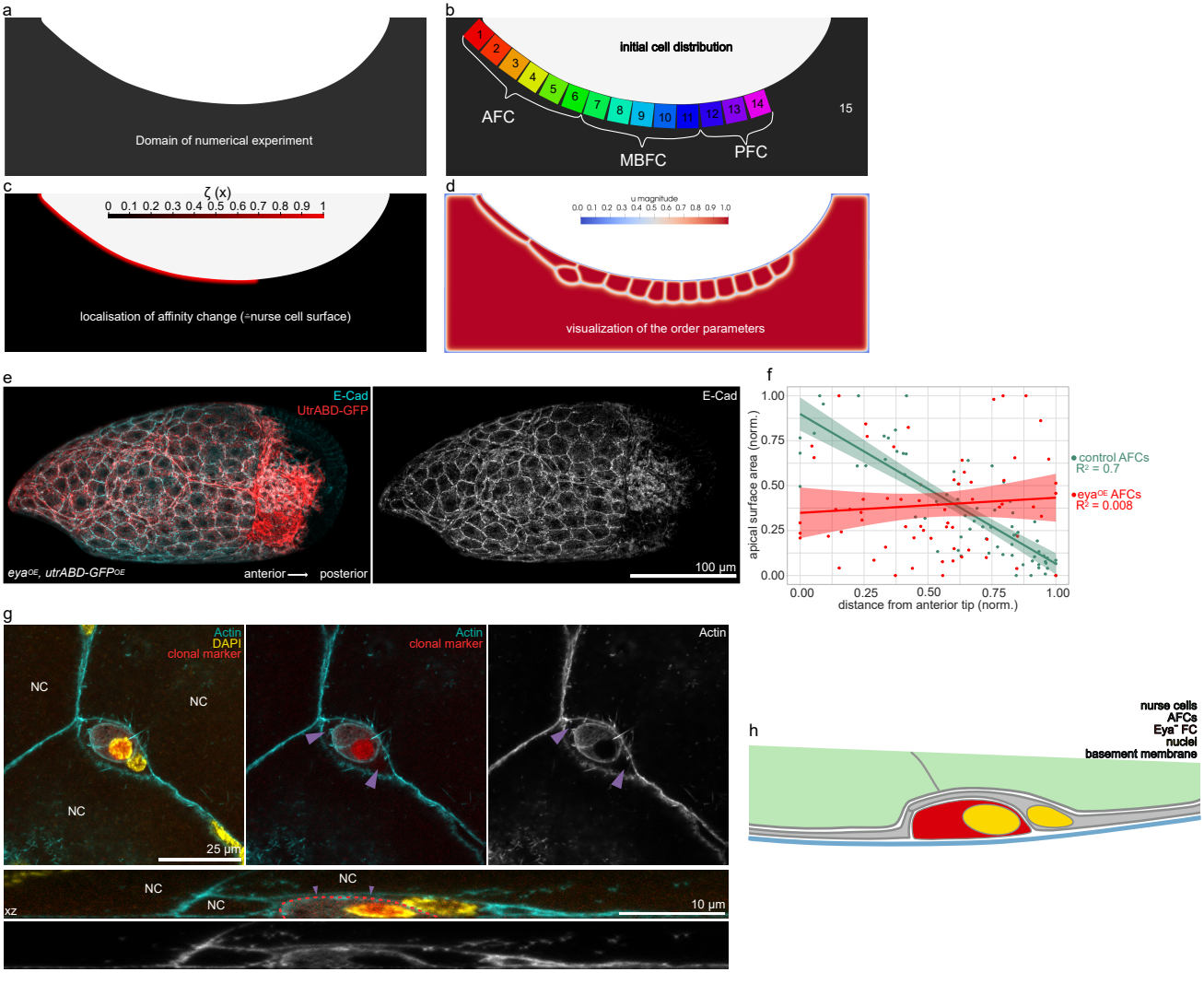
a
Domain of numerical experiment
b
initial cell distribution
1
2
3
4
5
6
7
8
9
10
11
12
13
14
15
AFC
MBFC
PFC
c
ζ (x)
0 0.1 0.2 0.3 0.4 0.5 0.6 0.7 0.8 0.9 1
localisation of affinity change (=nurse cell surface)
d
u magnitude
0.0 0.1 0.2 0.3 0.4 0.5 0.6 0.7 0.8 0.9 1.0
visualization of the order parameters
e
E-Cad
UtrABD-GFP
eyaOE, utrABD-GFPOE
anterior
posterior
E-Cad
100 µm
f
apical surface area (norm.)
1.00
0.75
0.50
0.25
0.00
0.00
0.25
0.50
0.75
1.00
distance from anterior tip (norm.)
control AFCs
R² = 0.7
eyaOE AFCs
R² = 0.008
g
Actin
DAPI
clonal marker
NC
NC
NC
25 µm
Actin
clonal marker
Actin
NC
NC
NC
xz
10 µm
h
nurse cells
AFCs
Eya- FC
nuclei
basement membrane

Supplementary Figure 4

Affinity-controlled FC interaction with the germline drives FC shapes and movements

a, Domain of computation Ω of the numerical experiment for the phase field model.
b, Initial cell distribution in the phase field model. Cells numbered from anterior to posterior.
c, Localization of the affinity change that represents the nurse cell surface.
d, Visualization of the order parameters of the phase field simulation.
e, Maximum fluorescence intensity projection of an egg chamber with clonal expression of *eya*^{OE} and *utrABD-gfp*, stained for E-Cad. Note how the gradient in apical surface areas of AFCs is lost upon broad overexpression of *eya*^{OE}.
f, Quantification of apical areas of AFCs as a function of their distance to the anterior tip for control AFCs and *eya*^{OE} AFCs. Linear regression with 95% CI area. n (control FCs: 71 FC, 3 EC; *eya*^{OE} FCs: 65 FC, 3 EC)
g, AFCs with clonal *eya-RNAi* expression of a phase 3 egg chamber, stained for F-Actin and nuclei (DAPI). One AFC is expressing *eya-RNAi* (red). *Eya-RNAi* expressing AFC (red dotted line) is rounded up and disconnected from nurse cells (NC). Wild type AFC extends between *eya-RNAi* AFC and nurse cells (purple arrowheads). Confocal section and xz-reslice shown.
h, Illustration of an AFC lacking Eya in a phase 3 egg chamber. The Eya-negative AFC is displaced from the nurse cell surface by wild type AFCs.
See Supplementary Table 7 for detailed statistical information. Source data are provided as a Source Data file.

Figure S5

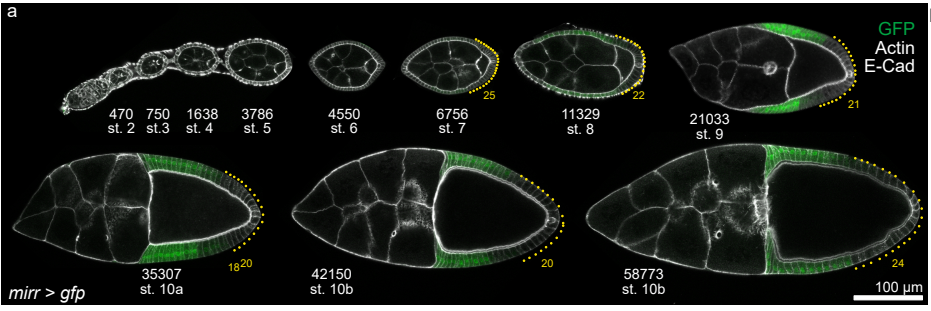
a
GFP
Actin
E-Cad
470
st. 2
750
st.3
1638
st. 4
3786
st. 5
4550
st. 6
6756
st. 7
11329
st. 8
21033
st. 9
35307
st. 10a
42150
st. 10b
58773
st. 10b
mirr > gfp
100 µm

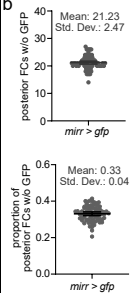
b
Mean: 21.23
Std. Dev.: 2.47
posterior FCs w/o GFP
mirr > gfp
Mean: 0.33
Std. Dev.: 0.04
proportion of posterior FCs w/o GFP
mirr > gfp

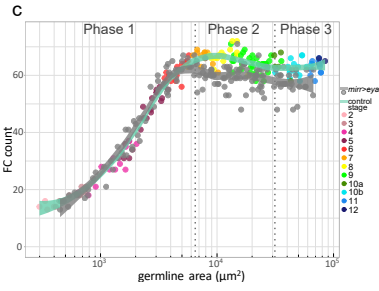
c
Phase 1
Phase 2
Phase 3
FC count
germline area (µm²)
mirr>eya
control stage

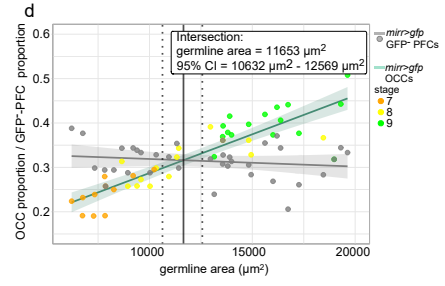
d
Intersection:
germline area = 11653 µm²
95% CI = 10632 µm² - 12569 µm²
mirr>gfp GFP⁻ PFCs
mirr>gfp OCCs
stage
OCC proportion / GFP⁻-PFC proportion
germline area (µm²)

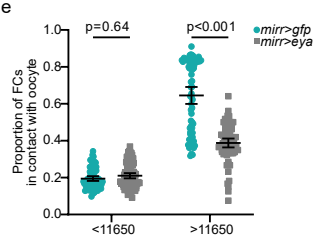
e
p=0.64
p<0.001
mirr>gfp
mirr>eya
Proportion of FCs in contact with oocyte
<11650
>11650

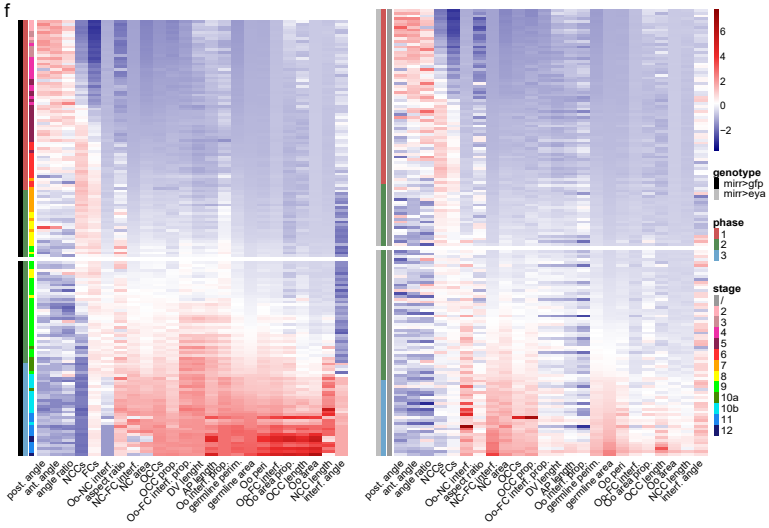
f
genotype
mirr>gfp
mirr>eya
phase
stage
post. angle
ant. angle
angle ratio
NC FCs
Oo-NC interf. ratio
aspect ratio
NC-FC interf. ratio
NC area
OCC FCs
OCC prop.
Oo-FC interf. prop.
DV length
AP length
germline perim.
germline area
Oo peri.
Oo aspect ratio
Oo area
OCC length
Oo length
NCC length
interf. angle

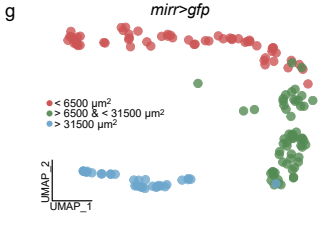
g
mirr>gfp
< 6500 µm²
> 6500 & < 31500 µm²
> 31500 µm²
UMAP_2
UMAP_1

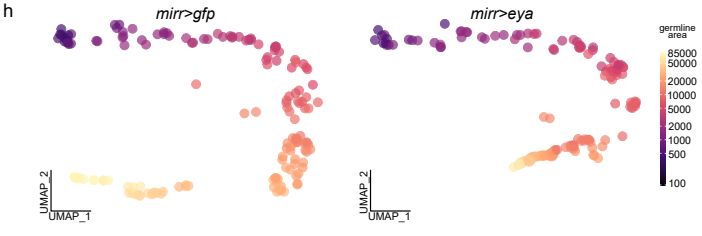
h
mirr>gfp
mirr>eya
germline area
UMAP_2
UMAP_1

Supplementary Figure 5

Ectopic Eya expression in MBFCs during phase 2 inhibits MBFC transition onto the oocyte

a, Medial confocal sections of egg chambers expressing *gfp* under the control of *mirr-GAL4* (*mirr>gfp*, MBFC driver), stained for F-Actin and E-Cad. Yellow dots mark posterior cells that are not under the control of *mirr-GAL4*. Numbers denote germline areas in μm^2.
b, Quantification of posterior cells without GFP as total cell count and as proportion of all FCs. Mean+95% CI, n = 80 EC.
c, FC count as a function of germline area for *mirr>gfp* and *mirr>eya^{OE}* egg chambers. LOESS fitted curves with 95% CI area.
d, Determining the 'critical size' as the germline area at which first GFP-positive FCs are expected to come into contact with the oocyte. *mirr>gfp* egg chambers with germline areas > 6500 μm^2 and < 20000 μm^2 were used. Linear regression between the proportion of FCs in contact with the oocyte (OCC=oocyte contacting FCs) and the proportion of posterior FCs without GFP (GFP-negative PFCs) was performed. Crossing point of the two linear regression curves was fitted. Linear regression +95% CI area shown. Solid grey line marks germline area at estimated intersection point and dotted grey lines mark 95% CI of the intersection germline area. See Supp. File S2 for detailed statistical information.
e, Parameter comparison between *mirr>gfp* and *mirr>eya* egg chambers grouped by germline area into smaller and larger than critical size (11650 μm^2). Mean +95% CI, two-way Anova with Šídák's multiple comparisons test; n (*mirr>gfp* (<11650 μm^2): 74 EC, *mirr>gfp* (>11650 μm^2): 74 EC, *mirr> eya^{OE}* (<11650 μm^2): 86 EC, *mirr> eya^{OE}* (>11650 μm^2): 71 EC).
f, Heatmap of the 24 morphological parameters of *mirr>gfp* and *mirr>eya^{OE}* egg chambers. Each row represents an individual egg chamber with increasing germline areas from top to bottom. Break in heatmap marks critical size (11650 μm^2). n (*mirr>gfp*: 153 egg chambers, *mirr>eya*^{OE}: 157 egg chambers).
g, UMAP plot depicting *mirr>gfp* egg chambers coloured based on their phase affiliation.
h, UMAP plot of *mirr>gfp* and *mirr>eya^{OE}* egg chambers coloured by their germline area.
See Supplementary Table 7 for detailed statistical information. Source data are provided as a Source Data file.

Figure S6

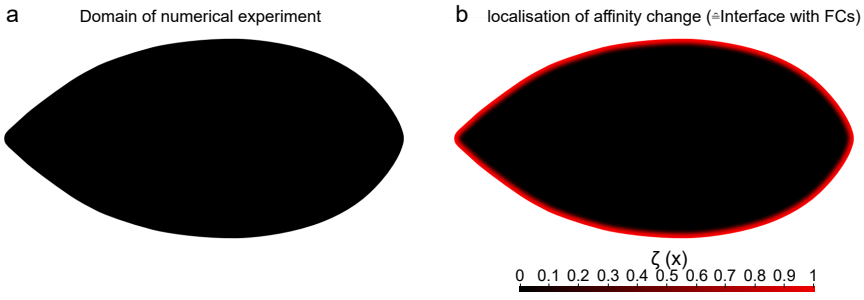
a
Domain of numerical experiment
b
localisation of affinity change (≙Interface with FCs)
ζ (x)
0 0.1 0.2 0.3 0.4 0.5 0.6 0.7 0.8 0.9 1

Supplementary Figure 6

Phase Field Model of Germline Cell Behaviour as a Function of their Effective Affinity for the Follicle Epithelium

a, Domain of computation Ω of the numerical experiment for the phase field model.
b, Localization of the affinity change that represents the nurse cell surface.

Figure S7

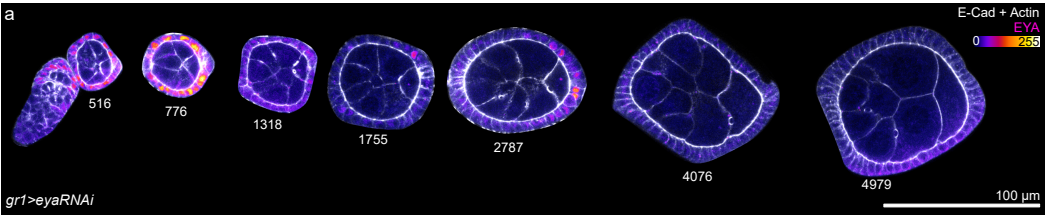
a
E-Cad + Actin
EYA
0
255
516
776
1318
1755
2787
4076
4979
gr1>eyaRNAi
100 µm

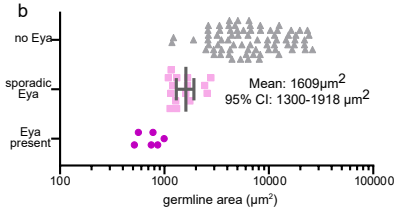
b
no Eya
sporadic Eya
Eya present
Mean: 1609µm2
95% CI: 1300-1918 µm2
100
1000
10000
100000
germline area (µm2)

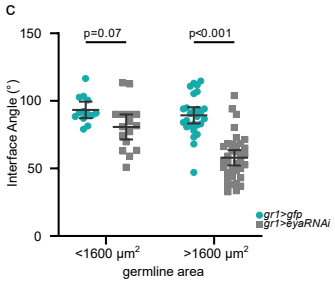
c
p=0.07
p<0.001
Interface Angle (°)
gr1>gfp
gr1>eyaRNAi
<1600 µm2
>1600 µm2
germline area

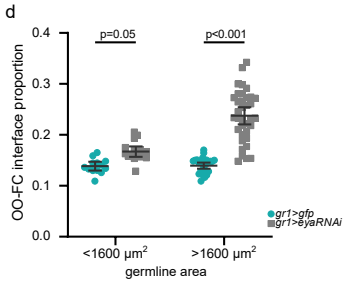
d
p=0.05
p<0.001
OO-FC interface proportion
gr1>gfp
gr1>eyaRNAi
<1600 µm2
>1600 µm2
germline area

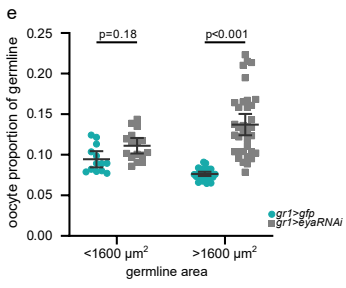
e
p=0.18
p<0.001
oocyte proportion of germline
gr1>gfp
gr1>eyaRNAi
<1600 µm2
>1600 µm2
germline area

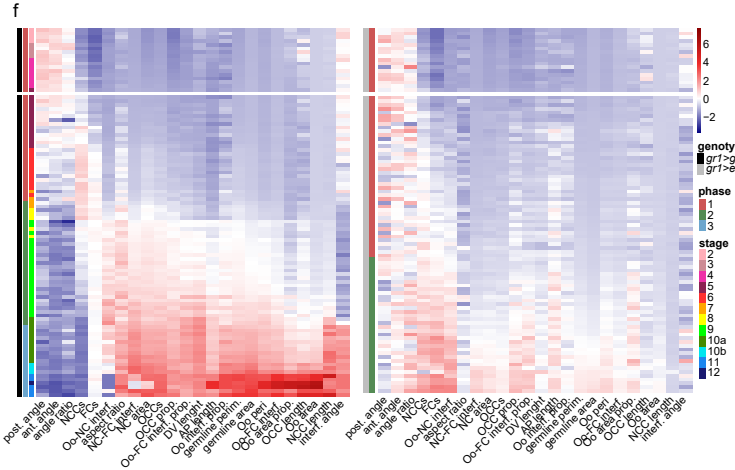
f
genotype
gr1>gfp
gr1>eyaRNA
phase
stage
post. angle
ant. angle
angle ratio
NC PCs
Oo-NC interf.
angle ratio
NC-FC interf.
NC area
OO-FC interf. prop.
DV length
AP length
germline perim
germline area
OC peri
OO-FC interf.
OO-FC length
OO area
NCC length
interf. angle

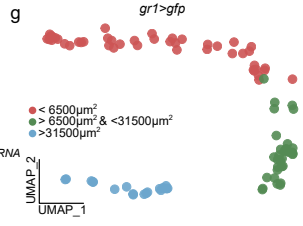
g
gr1>gfp
< 6500µm2
> 6500µm2 & <31500µm2
>31500µm2
UMAP_2
UMAP_1

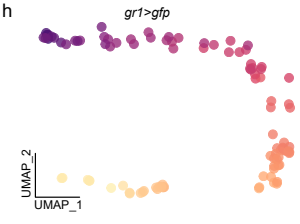
h
gr1>gfp
UMAP_2
UMAP_1

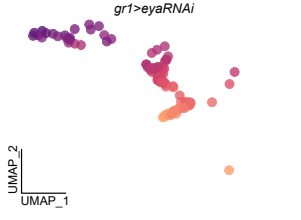
gr1>eyaRNAi
germline area
UMAP_2
UMAP_1

Supplementary Figure 7

Premature loss of Eya during phase 1 disrupts egg chamber morphogenesis

a, Medial confocal sections of egg chambers expressing *eya-RNAi* under the control of *gr1-GAL4* (*gr1>eya-RNAi*, FC driver), stained for F-Actin, E-Cad and Eya. Numbers denote germline area.
b, Quantification of Eya expression in FCs. Egg chambers were grouped into three categories (Eya present, sporadic Eya and no Eya in FCs) and plotted against their germline area. Mean+95%CI of the sporadic Eya group was determined as critical size from which on effects of *eya-RNAi* expression could be expected. Mean+95% CI, n (Eya present: 6 EC, sporadic Eya: 15 EC, no Eya: 75 EC).
c,d,e, Parameter comparison between *gr1>gfp* and *gr1>eya-RNAi* egg chambers for phase 1 (germline area < 6500 µm^2). Egg chambers grouped into smaller and larger than critical germline area (1600 µm^2). **c,** Interface Angle. **d,** Oocyte-FC interface proportion of germline-FC interface. **e,** Oocyte area proportion of germline area. Mean+95% CI, two-way Anova with Šídák's multiple comparisons test; n (*gr1>gfp* (<1600 µm^2): 13 EC, *gr1>gfp* (>1600 µm^2): 27 EC, *gr1>eya-RNAi* (<1600 µm^2): 16 EC, *gr1>eya-RNAi* (>1600 µm^2): 36 EC).
f, Heatmap of the 24 morphological parameters of *gr1>gfp* and *gr1>eya-RNAi* egg chambers. Each row represents an individual egg chamber with increasing germline areas from top to bottom. Note that no egg chambers of *gr1>eya-RNAi* exist with germline sizes corresponding to phase 3, as they degenerate before. Break in heatmap marks critical size (1600 µm^2). n (*gr1>gfp*: 97 EC, *gr1>eya-RNAi*: 96 EC).
g, UMAP plot of *gr1>gfp* egg chambers coloured based on their phase affiliation.
h, UMAP plot of *gr1>gfp* and *gr1>eya-RNAi* egg chambers coloured by their germline area size.
See Supplementary Table 7 for detailed statistical information. Source data are provided as a Source Data file.

Figure S8

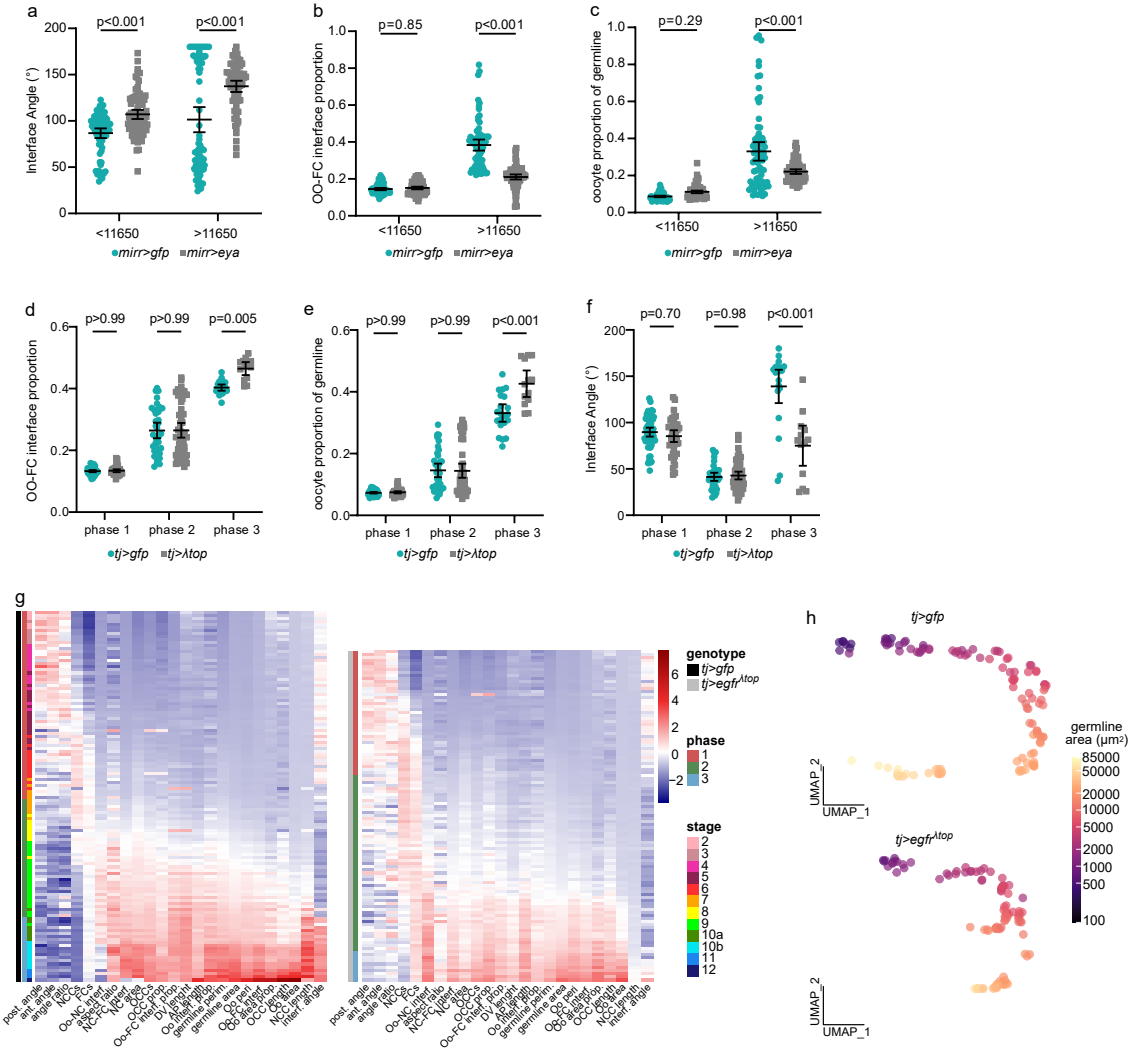
a
p<0.001
p<0.001
Interface Angle (°)
<11650
>11650
mirr>gfp
mirr>eya
b
p=0.85
p<0.001
OO-FC interface proportion
c
p=0.29
p<0.001
oocyte proportion of germline
d
p>0.99
p>0.99
p=0.005
phase 1
phase 2
phase 3
tj>gfp
tj>λtop
e
p>0.99
p>0.99
p<0.001
f
p=0.70
p=0.98
p<0.001
g
genotype
tj>gfp
tj>egfr^λtop
phase
stage
h
tj>gfp
tj>egfr^λtop
UMAP_1
UMAP_2
germline area (µm²)

Supplementary Figure 8

Manipulating Eya expression patterns during phase 2 and 3 disrupts oocyte expansion dynamics

a,b,c, Parameter comparison between *mirr>gfp* and *mirr>eya^{OE}* egg chambers. Egg chambers grouped into smaller and larger than critical germline area (11650 µm^2). **a,** Interface Angle. **b,** Oocyte-FC interface proportion of germline-FC interface. **c,** Oocyte area proportion of germline area. Mean+95% CI, two-way Anova with Šídák's multiple comparisons test; n (*mirr>gfp* (<11650 µm^2): 74 EC, *mirr>gfp* (>11650 µm^2): 74 EC, *mirr>eya^{OE}* (<11650 µm^2): 86 EC, *mirr>eya^{OE}* (>11650 µm^2): 71 EC).
d,e,f Parameter comparison between *tj>gfp* and *tj>egfr$^{\lambda top}$* egg chambers. Egg chambers subdivided by phases. **d,** Interface Angle. **e,** Oocyte-FC interface proportion of germline-FC interface. **f,** Oocyte area proportion of germline area. Mean+95% CI, two-way Anova with Šídák's multiple comparisons test; n (*tj>gfp* (phase 1): 62 EC, *tj>gfp* (phase 2): 39 EC, *tj>gfp* (phase 3): 21 EC, *tj>egfr$^{\lambda top}$* (phase 1): 41 EC, *tj>egfr$^{\lambda top}$* (phase 2): 58 EC, *tj>egfr$^{\lambda top}$* (phase 3): 10 EC). See Supp. File S2 for detailed statistical information.
g, Heatmap of the 24 morphological parameters of *tj>gfp* and *tj>egfr$^{\lambda top}$* egg chambers. Each row represents an individual egg chamber with increasing germline areas from top to bottom. n (*tj>gfp*: 122 EC, *tj>egfr$^{\lambda top}$*: 109 EC).
h, UMAP plot of *tj>gfp* and *tj>egfr$^{\lambda top}$* egg chambers coloured based on germline area size.
See Supplementary Table 7 for detailed statistical information. Source data are provided as a Source Data file.

Supplementary Note: Phase Field Model

Based on classical work[1], we formulated a phase field model to describe the collective behavior of follicle cells (FCs) – or, in a separate simulation, the behavior of the oocyte and nurse cells – as their relative affinity to the germline surface or the FC surface, respectively, changes. Nomoura[2] used phase fields to describe multicellular systems. Moure and Gomez[3] provide a recent overview of the application of phase field models to study the migration of individual cells and their collective behavior. Wenzel and Voigt[4] consider collective cell migration. Phase field models have furthermore been successfully applied in, e.g., tumor growth modeling[5,6]. The ideas therein are similar to the use of such models for grain boundary evolution in polycrystalline materials[7,8]. In the spirit of Modica and Mortola[9], we consider the phase field model as a diffuse approximation for a sharp interface model, where each cell is subject to a surface tension, exhibits a prescribed affinity to a defined part of the boundary, and must satisfy a number of constraints.

Set-up of the model. Roughly following work for grain boundary evolution[7], we start with an energy of the form

$$F(u,x,t) = \int_\Omega f(u_1(x), u_2(x), \dots, u_N(x), x, t) + \sum_{j=1}^{N} \frac{\kappa_j}{2} |\nabla u_j|^2 \,\mathrm{d}x, \tag{1}$$

associated to a vector valued order parameter field $u = (u_1, u_2, \dots, u_N)$ defined on a domain $\Omega \subset \mathbb{R}^2$, describing N cells, where the function f is given as

$$f(u,x,t) = \sum_{j=1}^{N} \phi_j(x,t) \left(-\frac{\alpha}{2} u_j^2 + \frac{\beta}{4} u_j^2 \right) \tag{2}$$

$$+ \gamma \sum_{j=1}^{N} \sum_{i=j+1}^{N} u_i^2 u_j^2 \tag{3}$$

for constants $\kappa_j > 0$, $\alpha > 0$, $\beta > 0$, $\gamma > 0$ and functions $\phi_j(x,t)$. It should be noted that, as long as $2\gamma > \phi_j(x,t)\beta$, the function f is locally minimized exactly at the "pure phases" $u_j = \pm 1$, $u_i = 0$ if $i \neq j$. For ϕ_j independent of j, these minimizers are degenerate, otherwise minimizers for which the corresponding ϕ_j is larger are energetically favored. Each one of these pure phases denotes the position of a given cell, i.e., the set $\{u \approx (0, \dots, 0, 1, 0, \dots, 0)\}$, with the entry 1 in the j-th component of the vector is the part of the domain Ω occupied by cell number j. Our experiments are conducted such that the negative minima are not seen by the simulation.

In our phase field simulation, we compute the L^2-gradient flow of the time dependent energy F, thus solving

$$\mu \dot{u}_j = -\phi_j(x,t) \left(-\alpha u_j + \beta u_j^3 \right) - 2\gamma \left(\sum_{i \neq j} u_i^2 \right) u_j + \kappa_j \Delta u_j, \tag{4}$$

given an initial condition $u^{(0)}(x) = \left(u_1^{(0)}(x), \dots, u_N^{(0)}(x) \right)$ describing the starting arrangement of cells and boundary conditions $u(\cdot,t) = 0$ on $\partial\Omega$ for all $t \geq 0$. Above, $\dot{u}_j$ denotes the time derivative of u_j and Δ is the Laplace-operator. The constant $\mu > 0$ denotes the time-scale. For a subset

Table S7: Polynomial coefficients for $\phi_j(t) = \sum_{k=0}^{6} a_{jk} t^k$.

	a_{j0}	a_{j1}	a_{j2}	a_{j3}	a_{j4}	a_{j5}	a_{j6}
Row $j = 1$	7.22519	0	-77.5944	279.897	-398.117	276.264	-78.7263
Row $j = 2$	6.99944	0	-95.0403	458.222	-905.773	836.279	-290.315
Row $j = 3$	6.82173	0	-65.7434	295.514	-588.111	576.878	-214.334
Row $j = 4$	6.48935	0	-47.8079	243.145	-605.621	707.857	-291.604
Row $j = 5$	7.02846	0	-96.7535	521.399	-1246.33	1351.44	-523.595
Row $j = 6$	6.65126	0	-24.4169	-5.49423	91.6108	-72.3666	10.2843
Row $j = 7$	6.79833	0	-79.8118	304.779	-528.733	433.352	-134.256

of cells we constrain this gradient flow to be area preserving, i.e.,

$$\int_\Omega u_j(x,t)\,\mathrm{d}x = \int_\Omega u_j^{(0)}(x)\,\mathrm{d}x \quad \text{for all } t > 0 \text{ and } j \in J_{\text{vol}} \subset \{1,\dots,N\}, \tag{5}$$

where J_{vol} simply denotes the subset of cells for which volume preservation is enabled.

Follicle cells simulation. The numerical experiments are performed on a domain resembling the exterior of the germline at stage 10a, see Fig. S4a (in the supplementary materials), which is the rectangle $(-2,2)\times(0,1.5)$ minus the space occupied by the germline. The initial cell distribution is given as seen in Fig. S4b, where (from left-to-right), the individual colors denote individual cells (cells 1 through 14).

In our simulation, cells 1–6 represent AFCs, where cell 6 is a centripetal cell. Cells 7–11 are MBFCs, and 12–14 PFCs. We reduced the number of FCs since MBFCs and PFCs share similar affinity dynamics.

The gray background is assigned to "cell" $N = 15$. On the area occupied by cell j we then simply set $u_j^{(0)} = 1$, zero outside that area. Area preservation during the evolution is enforced for cells 1 through 14, but not for cell 15 (for which it is automatically preserved as the remaining area of Ω). For all experiments, we first relax the initial condition by simulating the evolution equation with the initial $\phi_j(x,0)$ until an equilibrium was reached.

To simulate the changing affinity of the individual FCs' apical surface to the nurse cells, we increase the function $\phi_j(x,t)$ in the vicinity of the nurse cells' surface – this makes it energetically favorable for cell j to concentrate its volume near the apical surface. More precisely, we fix a function $\zeta(x) \in [0,1]$ on Ω, as seen in Fig. S4c and set $\phi_j(x,t) = \hat{\phi}_j(t)\zeta(x) + 2(1-\zeta(x))$. In the sense of a sharp interface limit, this change near the boundary should be seen as an affinity changing boundary condition for the phase field variables.

In all experiments, the time-scale μ, which fixes the relaxation time relative to the time-scale on which $\hat{\phi}_j(t)$ changes, is set to $\mu = 1.1125 \cdot 10^{-3}$ hours. The further constants are $\alpha = \beta = 1$, $\gamma = 20$ and $\kappa_j = 3 \cdot 10^{-4}$ for $j \neq 15$, and $\kappa_{15} = 6 \cdot 10^{-4}$.

For the experiment recreating the wild-type situation, we fix $\hat{\phi}_j(t)$ for cells $j = 1$–7 (from left to right) corresponding to rows 1–7 in Fig. 4d. All other cells are set to the affinity of row 7, up to cell 15. The affinities were generated from averaged measured EYA levels (normalized to lie between 2 and 12, shown as circles in Fig. 4c) using least squares approximation by a sixth-order polynomial $\phi_j(t) = \sum_{k=0}^{6} a_{jk} t^k$ constrained to have vanishing derivative at $t = 0$ and $t = 36$ hours. The coefficients can be found in Table S7.

A number of further numerical simulations with 15 cells, corresponding to experiments, were conducted.

- For the experiment with equal affinities we set the affinities $\hat{\phi}_j(t)$ of all cells 1–15 constant to that of row 1 at $t = 0$.
- Simulating the behavior with absent affinity gradient in AFCs, we set the affinity for cells 1–6 to that of row 1. Cells 7–15 receive the affinity of row 7. The time-dependent behaviors of $\hat{\phi}_1(t)$ and $\hat{\phi}_7(t)$ are not changed here.
- In the experiment where the third cell is assigned a lower affinity, the setting is equal to the wild-type experiment, except that cell 3 is assigned the lower affinity of row 7.
- To simulate the ectopic affinity increase in MBFCs, we assign affinities of row 1–5 to AFCs 1–5 as usual. Centripetal cell 6, as well as MBFCs 7 and 8, however, receive the increased affinity of row 2. All other cells receive the affinity of row 7, as usual.

Rectangular domain. To further examine the shape of adjacent cells, an experiment with three square cells on a rectangle $(0, 1.5) \times (0, 0.5)$ was performed. All parameters were chosen as in the above described simulations. On the rectangle, we set $\zeta(x) = \left(1 - \frac{x_2}{10}\right)^+ = \max\left\{0, 1 - \frac{x_2}{10}\right\}$. For the experiment showing the polarization of cell motion, we set $\hat{\phi}_j(t)$ for the three cells to the affinities of rows 5, 6, and 7, from left to right. For the experiment with symmetric affinities we used rows 7, 5, and again 7.

Oocyte and nurse cells. Finally, the interior of the egg chamber, i.e., the oocyte and the nurse cells, were simulated on a suitable domain (essentially the complement of the domain for the FCs simulation, see Fig. S6a). The nurse cells were considered collectively as one "cell", $j = 1$, and the oocyte is cell $j = 2$ (thus a total of $N = 2$ cells). In this experiment, we set $\kappa_j = 5 \cdot 10^{-4}$ for all j. The initial condition was set such that 84% of the total length of the domain is covered by the nurse cells - this initial condition is allowed to relax before the start of stage 5. Again, the affinity towards the surface of the germline was modulated again by making the functions ϕ_j space- and time dependent. For this experiment, we chose

$$\phi_1(x,t) = \zeta(x)\hat{\phi}_1(x,t), \tag{6}$$

$$\phi_2(x,t) = \zeta(x)\hat{\phi}_2(x,t) + p + p_{\text{constr}}(v), \tag{7}$$

where ζ (shown in Fig. S6b) is again the cutoff function to ensure the changed affinity is only applied at the surface. Furthermore, we add a constant pressure $p = 6.5 \cdot 10^{-2}$ and an oocyte volume v dependent pressure $p_{\text{constr}}(v) = \frac{7 \cdot 10^{-3}}{v - 7 \cdot 10^{-2}}$ to the oocyte model, noting that the total area of the computational domain is 3.96. These terms model oocyte growth effects due to transport of matter by the nurse cells as well as a minimal volume cutoff for the oocyte.

The now space- and time-dependent functions $\hat{\phi}_j(x,t)$ are given as follows. First, the relative affinity $\iota(x,t)$ of FCs at different points on the boundary is computed by evaluating which cell row $j = 1, \ldots, 7$ is occupying which point on the boundary, and then evaluating the respective relative affinity of that cell row by the polynomial expression as in the previous experiment. The centers of the cell positions are measured by experiment and then fit using a cubic polynomial with coefficients given in Table S8, where a position of 0 denotes the anterior end of the germline and 1 denotes the posterior end. The positions and measured values are illustrated in Fig. 6 j&k, and we assume that each cell occupies the space up to the mid point between itself and its neighbor (or up to the ends for the first and the last cell). We remark that "cell" 7 again encompasses a number of cells towards the posterior end, which all have comparable Eya expression. From the relative affinity we then compute the oocyte and nurse cell affinity as

Table S8: Polynomial coefficients for the cell position centers $\sum_{k=0}^{5} b_{jk} t^k$.

	b_{j0}	b_{j1}	b_{j2}	b_{j3}	b_{j4}	b_{j5}
Row $j=1$	0.069791	0	-0.63461	3.28734	-4.76849	2.09623
Row $j=2$	0.128197	0	-2.09907	8.93208	-11.334	4.54757
Row $j=3$	0.189402	0	-2.93928	11.7103	-14.0911	5.4224
Row $j=4$	0.224447	0	-2.83186	11.2882	-13.2071	4.92549
Row $j=5$	0.261511	0	-2.69858	10.2531	-11.154	3.85078
Row $j=6$	0.313222	0	-2.98772	10.8291	-11.3885	3.80847
Row $j=7$	0.361412	0	-3.41095	12.3623	-13.3566	4.63224

$\hat{\phi}_1(x,t) = 2.0 + 0.7(\imath(x,t) - 5.7120)^+$ and $\hat{\phi}_2(x,t) = 2.0 + 0.7(5.7120 - \imath(x,t))^+$, respectively, where the cutoff of 5.7120 corresponds to an Eya fluorescence intensity of 72. Again, the superscript "+" denotes taking the positive part of a term. Note that in figures we simply show the function $0.7(5.7120 - \imath(x,t))$, so that positive values indicate increased oocyte affinity, and negative values indicate increased nurse cell affinity. Fig. 6j shows for which FC row at what time nurse cell and oocyte contact are preferred, respectively. The transitions between constant affinities were smoothed by an affine transition layer of width 0.05.

One further change compared to the simulations of the exterior of the germline concerns the change of volume of the involved cells. Here, the volumes of the nurse cells and the oocyte are not fixed, but the in each time step only a fraction of $8 \cdot 10^{-4}$ of the unconstrained volume change for the oocyte is allowed, simulating the limited volume exchange through ring canals. This is implemented by first solving the unconstrained problem and then constraining the new volume using a Lagrange multiplier.

Again, a number of further simulations, corresponding to experiments, were conducted.

- Oocyte affinity was set high on the entire surface starting already from stage 5. This recapitulates a premature loss of Eya during phase 1.
- Nurse cell affinity was set high on 80% of the surface, and oocyte affinity is high only on 20% of the surface starting stage 6. This simulated ectopic effective nurse cell affinity in the region of MBFCs.
- Oocyte affinity was increased on the entire surface from stage 6, creating an entirely Eya-negative follicle epithelium during phase 2.

Further simulation and visualization details. All numerical experiments were conducted using the finite element method. For the exterior of the germline, Ω was discretized using P1 finite elements on a uniform tesselation with 92 321 triangles (for a domain volume of 4.03), on the rectangular domain we used 68 887 triangles (for a domain volume of 0.75) and for the interior of the germline Ω was discretized using 62 968 triangles (for a domain volume of 3.96). The time-discretization was semi-implicit with a time-step size of $5.625 \cdot 10^{-5}$ hours. For visualization, we show the sets $u_j \geq 0.3$, $j = 1, \dots, 14$ (or $j = 1, \dots, 3$ for the rectangular domain), smoothly cut off and colored by the respective cell's affinity. Each (multi-threaded) simulation requires between 6 hours and two days of wall time (depending on the number of phase field variables considered) on an Intel Xeon Gold 6230. For visualization of the interior of the germline, the nurse cells and the oocyte were colored in light and dark green, respectively, with the affinity visualized by the color in a band around the germline. For an example of a more direct visualization of the order parameters, see Fig. S4d, where the value $\left(\sum_{j=1}^{N} u_j^2\right)^{\frac{1}{2}}$

is plotted for the experiment with modified cell 3 affinity. For creating the images, the software Paraview 5.10.1[10,11] was used.

Supplementary Tables 1-7

Supplementary Table 1 - Fly strains

Fly line	Chromosome	Source
w[118]	*X*	David Bilder
hsflp[1]	*I*	BDSC 6
hsflp[122]	*I*	Iswar Hariharan
act>y[+]>-GAL4,UAS-RFP/TM6c	*III*	BDSC 30558
act>y[+]>-GAL4,UAS-GFP/TM6b	*I,III*	Bruce A. Edgar
FRT42D ubi-eGFP/CyO	*I,II*	BDSC 5626
Act5C.GAL4 (FRT.CD2), UASp-UtrABD-eGFP /TM6c	*III*	BDSC 4780 & Katja Röper (recombined in this study)
tubGAL80[ts]-20; TM2/TM6b	*II,III*	BDSC 7019
Sco/CyO; tub-GAL80[ts]-7	*II,III*	BDSC 7018
c306-GAL4	*X*	BDSC 3743
tj-GAL4, Mef2-GAL80/CyO	*II*	Sally Horne-Badovinac
tj-GAL4, UAS-CD8tom/CyO; UAS-dcr2/TM6C	*II,III*	David Bilder
MTD-GAL4 (Otu-Gal4::VP16;nos-GAL4;nos-GAL4::VP16)	*I,II,III*	BDSC 31777
mirr-GAL4/TM3, Sb[1]	*III*	BDSC 29650
tub-GAL80[ts]-20/Cyo; fru-GAL4/TM6(hu)	*II,III*	Vincent Mirouse
matalpha-GAL-VP16	*III*	BDSC 7063
GR1-Gal4	*III*	BDSC 36287
PG150-GAL4/FM7a	*I*	Kim McCall
UASp-UtrABD-eGFP	*III*	Thomas Lecuit
UAS-upd1 / CyO,ubi-GFP	*II*	Martin Zeidler
UAS-Dl RNAi (GL000520)	*II*	BDSC 36784
UAS-hts-mCherry	*III*	BDSC 66171
UAS-eya	*III*	BDSC 5675

UAS-eya RNAi (HMS04515)	*II*	BDSC 57314
FRT42D shg [R69b]/ SM6b, cn#1	*II*	Ulrich Tepass
UAS-shg RNAi (HMS00693)	*III*	BDSC 32904
UAS-shg RNAi (GL00646)	*II*	BDSC 38207
UAS-CadN RNAi (1093/GD)	*II*	VDRC1093
UAS-hpo	*II*	Barry Thompson
UAS-GFP (S56T) /CyO	*II*	BDSC 1521
UAS-mCD8::RFP	*II*	BDSC 32219
UAS-egfr$^{\lambda top}$	*III*	BDSC 59843

Supplementary Table 2 - Experimental genotypes

Figure	Genotype
Figure 1	
a - g	*w[118]*
Figure S1	
b	*w[118]*
Figure 2	
c - f	*tj-GAL4, UAS-CD8tom/+ ; UAS-dcr2/UASp-UtrABD-eGFP*
g,h	*w[118]*
j	*hsflp[122] /+; UAS-upd1/Sp; act>y[+]>-GAL4,UAS-GFP/+*
k	*grk(2B6) b, cn, slbo/grk(2E12)*
l	*Otu-Gal4::VP16/+;nos-GAL4/UAS-Dl RNAi;nos-GAL4::VP16/+*
Figure S2	
a	*hsflp [122]/+; FRT42D ubi-eGFP/FRT42D-shg[R69b]*
b	*tj-GAL4, UAS-CD8tom /UAS-CadNRNAi; UAS-shg RNAi/UAS-Dcr2*
c	*hsflp [122] /+;UAS-hpo/+; act> y[+]>Gal4, UASp-UtrABD-eGFP/+*
d-f	*w[118]*
Figure 3	
a,b,g,h,l,m	*hsflp [122] /+;; act> y[+]>Gal4, UASp-UtrABD-eGFP /UAS-eya*
d,e	*hsflp [122] /+;; act> y[+]>Gal4, UASp-UtrABD-eGFP /UAS-eya RNAi*
j,o	*hsflp [122] /+;; act> y[+]>Gal4, UASp-UtrABD-eGFP /UAS-hts-mCherry*
p,q	*Tj-Gal4, mef2-Gal80/+ ; UAS-hts-mCherry/+*
r,u	*w[118]*
Figure S3	
b	*tj-GAL4, UAS-CD8tom/CyO; UAS-dcr2/TM6C*
c	*tj-GAL4, UAS-CD8tom/UAS-eyaRNAi; UAS-dcr2/+*
e	*tj-GAL4, UAS-CD8tom/CyO; UAS-dcr2/TM6C & tj-GAL4, UAS-CD8tom/UAS-eyaRNAi; UAS-dcr2/+*
Figure 4	
a, c, l	*w[118]*
b, e	*tj-GAL4, UAS-CD8tom/+ ; UAS-dcr2/UASp-UtrABD-eGFP*
i	*C306-GAL4/+; tub-GAL80[ts]-20/UAS-eya RNAi*
Figure S4	

f, g	*hsflp [122] /+;; act> y[+]>Gal4, UASp-UtrABD-eGFP /UAS-eya*
h	*hsflp[122]/+;UAS-eya RNAi/+; act>y[+]>-GAL4,UAS-RFP/+*
j	*tj-Gal4, mef2-Gal80/+ ; UAS-htsmCherry/+*
k	*w[118]*
l	*hsflp [122]/+; FRT42D ubi-eGFP/FRT42D-shg[R69b]*
Figure 5	
b,d	*tub-GAL80[ts]-20/ UAS-GFP (S56T); mirr-GAL4/+*
c,e	*tub-GAL80[ts]-20/ +; mirr-GAL4/UAS-eya*
f,g,h	*tub-GAL80[ts]-20/ UAS-GFP (S56T); mirr-GAL4/+ & tub-GAL80[ts]-20/ +; mirr-GAL4/UAS-eya*
Figure S5	
a, b, d, f	*tub-GAL80[ts]-20/ UAS-GFP (S56T); mirr-GAL4/+*
c, e, g, h	*tub-GAL80[ts]-20/ UAS-GFP (S56T); mirr-GAL4/+ & tub-GAL80[ts]-20/ +; mirr-GAL4/UAS-eya*
Figure 6	
c-k	*w[118]*
Figure 7	
e	*GR1-Gal4/ UAS-GFP (S56T)*
f	*GR1-Gal4/ UAS-eya RNAi*
g,i-n	*GR1-Gal4/ UAS-GFP (S56T) & GR1-Gal4/ UAS-eya RNAi*
Figure S7	
a, b	*GR1-Gal4/ UAS-eya RNAi*
d	*GR1-Gal4/ UAS-GFP (S56T)*
c, e, f, g, h	*GR1-Gal4/ UAS-GFP (S56T) (control) & GR1-Gal4/ UAS-eya RNAi*
Figure 8	
e	*tub-GAL80[ts]-20/ UAS-GFP (S56T); mirr-GAL4/+*
f	*tub-GAL80[ts]-20/ +; mirr-GAL4/UAS-eya*
g-j	*tub-GAL80[ts]-20/ UAS-GFP (S56T); mirr-GAL4/+ & tub-GAL80[ts]-20/ +; mirr-GAL4/UAS-eya*
Figure S8	
a - c	*tub-GAL80[ts]-20/ UAS-GFP (S56T); mirr-GAL4/+ & tub-GAL80[ts]-20/ +; mirr-GAL4/UAS-eya*
d - h	*tj-GAL4, UAS-CD8tom/UAS-GFP(S56T); UAS-dcr2/+ & tj-GAL4, UAS-CD8tom/+; UAS-dcr2/UAS-egfr$^{\lambda top}$*
Figure 9	

e	*tj-GAL4, UAS-CD8tom/UAS-GFP(S56T); UAS-dcr2/+*
f	*tj-GAL4, UAS-CD8tom/+; UAS-dcr2/UAS-egfr$^{\lambda top}$*
g-k	*tj-GAL4, UAS-CD8tom/UAS-GFP(S56T); UAS-dcr2/+ & tj-GAL4, UAS-CD8tom/+; UAS-dcr2/UAS-egfr$^{\lambda top}$*

Supplementary Table 3 - Morphological parameters

Parameters	**unit**	**Parameters**	**unit**
germline area	μm^2	FC in contact with oocyte (OCC)	count
oocyte area	μm^2	FC in contact with nurse cells (NCC)	count
nurse cell area	μm^2	total no. of FCs	count
oocyte proportion of germline (oocyte area/germline area)	-	OCC proportion (OCC/total FC)	-
FC-OO interface length	µm	av. OCC length	µm
OO-NC interface length	µm	av. NCC length	µm
FC-NC interface length	µm	AP axis length	µm
FC-OO interface proportion of FC interface (FC-OO interface length/ germline-FC interface length)	-	DV axis length	µm
OO perimeter	µm	angle of anterior egg chamber tip	°
germline-FC interface length	µm	angle of posterior egg chamber tip	°
FC-OO interface proportion of OO perimeter (FC-OO interface length/ OO perimeter)	-	aspect ratio (AP axis length/DV axis length)	-
angle at FC-OO-NC meeting point	°	tip angle ratio (angle of anterior egg chamber tip/ angle of posterior egg chamber tip)	-

Supplementary Table 4 - Genotypes and number of egg chambers quantified for UMAP analysis

genotype	N	genotype	N
Wild type (w^{1118})	126	*fru>gfp*	85
gr1>gfp	97	*fru>eyaRNAi*	81
gr1>eyaRNAi	96	*tj>gfp,cd8tom,dcr2*	122
mirr>gfp	153	*tj>cd8tom,dcr2,egfr$^{\lambda top}$*	109
mirr>eya	157		

Supplementary Table 5 - Germline area size bins for Phase 1, 2, 3

Phase	Germline size (µm^2)
1	≤ 6500
2	> 6500 & ≤ 31500
3	>31500

Supplementary Table 6 - Quantification parameters for morphology of individual nurse cells

NC morphology parameter	unit
NC area	µm^2
NC perimeter	µm
NC-FC interface length	µm
Nucleus area	µm^2
NC-FC interface proportion (NC-FC interface / NC perimeter)	-
NC area proportion (NC area / germline area)	-
Nucleus proportion (Nucleus area / NC area)	-

Supplementary Table 7 - Reproducibility and Statistics

Reproducibility Statement			
Wherever representative microscopy images are shown at least 5 fully independent experiments were performed (including independent genetic crosses).			
Figure 1 f,g,h			
Statistical Analysis	Local polynomial regression fitting (LOESS), descriptive statistics and linear regression with y ~ germline size		
Data	Genotype: *wt* (w^{1118}) Multidimensional egg chamber morphology dataset. Parameters plotted against germline size. Germline Sizes for phase assignment: Phase 1: <6500µm^2; Phase 2: >6500µm^2 & < 31500 µm^2; Phase 3: >31500 µm^2		
N	126 egg chambers manually selected to sufficiently cover egg chamber development from stage 2 to 12. Frequencies are not representative of population stage or size frequencies. Phase 1: 62, Phase 2: 39, Phase 3: 26		
Descriptive Statistics	Total cell count	OCC proportion	NC area
LOESS	Degree of polynomial: 2 Level of CI: 0.95 Size of neighbourhood for fitting: 0.5	Degree of polynomial: 2 Level of CI: 0.95 Size of neighbourhood for fitting: 0.4	Degree of polynomial: 2 Level of CI: 0.95 Size of neighbourhood for fitting: 0.25
Phase 1	Min: 13 Max: 66 Mean: 46.68 SD: 15.03 CV: 0.322	Min: 0.107 Max: 0.258 Mean: 0.1732 SD: 0.035 CV: 0.2	Min: 306 Max: 5375 Mean: 2652 SD: 1477 CV: 0.56
Phase 2	Min: 57 Max: 69 Mean: 61.82 SD: 2.752 CV: 0.045	Min: 0.2188 Max: 0.825 Mean: 0.4917 SD: 0.184 CV: 0.37	Min: 6043 Max: 20556 Mean: 10872 SD: 3570 CV: 0.33
Phase 3	Min: 52 Max: 64 Mean: 58.19 SD: 2.743 CV: 0.047	Min: 0.7869 Max: 0.907 Mean: 0.844 SD: 0.032 CV: 0.038	Min: 5214 Max: 32757 Mean: 21603 SD: 8557 CV: 0.4
Linear Regression	Phase 1 Slope: $8.5*10^{-3}$ Phase 2 Slope: $-1.5*10^{-4}$ Phase 3 Slope: $-5.53*10^{-5}$	Phase 1 Slope: $1.03*10^{-5}$ Phase 2 Slope: $2.96*10^{-5}$ Phase 3 Slope: $1.43*10^{-6}$	Phase 1 Slope: 0.9 Phase 2 Slope: 0.59 Phase 3 Slope: -0.38

Figure 2 f			
Statistical Analysis	Local polynomial regression fitting (LOESS)		
Data	Genotype: *tj>cd8tom,ubdABD-gfp* Nuclear Eya levels and apical surface areas of cells plotted as a function of their distance to the anterior pole.		
	Phase 1 (st. 4)	Phase 2 (st. 9)	Phase 3 (st. 10a&b)
N	2 egg chambers, 45 cells	3 egg chambers, 192 cells	3 egg chambers, 112 cells Subgrouped into high (intensity >50) Eya cells and low (intensity <50) Eya cells
Local polynomial regression fitting parameters	Degree of polynomial: 2 Level of CI: 0.95 Size of neighbourhood for fitting: 0.75	Degree of polynomial: 2 Level of CI: 0.95 Size of neighbourhood for fitting: 0.6	Degree of polynomial: 2 Level of CI: 0.95 Size of neighbourhood for fitting: 0.75

Figure 2g			
Statistical Analysis	Descriptive Analysis		
Data	Genotype: w^{1118} FC row count of rows in contact with nurse cells of individual egg chambers sub-grouped into phase 1, 2 and 3. For Phase 1 only egg chambers with completed FC proliferation were used.		
	Phase 1	Phase 2	Phase 3
N	11	32	12
Descriptive Statistics	Min: 20 Max: 23 Mean: 21.82 SD: 1.4 CV: 0.064	Min: 8 Max: 21 Mean: 15.81 SD: 3.5 CV: 0.222	Min: 6 Max: 7 Mean: 6.08 SD: 0.289 CV: 0.047

Figure 2h						
Statistical Analysis	Descriptive Statistics					
Data	Genotype: w^{1118} Mean Eya row intensities of Phase 3 (stage 10a and 10b) egg chambers.					
N	5 egg chambers					
Descriptive Statistics	Row 1 Min: 69.46 Max: 112.4 Mean: 92.66 SD: 17.95	Row 2 Min: 77.10 Max: 127.8 Mean: 101 SD: 18.98	Row 3 Min: 91.29 Max: 133.9 Mean: 105.8 SD: 16.88	Row 4 Min: 92.2 Max: 150 Mean: 114.4 SD: 21.66	Row 5 Min: 92.37 Max: 151.9 Mean: 115.4 SD: 22.14	Row 6 Min: 48.16 Max: 67.30 Mean: 62.40 SD: 8
	Row 7 Min: 16.39 Max: 23.14 Mean: 20.09 SD: 2.85	Pooled rows 8-26: Min: 6.27 Max: 23.47 Mean: 13.05 SD: 3.4				

Figure S2e									
Statistical Analysis	Regression fitting								
Data	Genotype: w^{1118} Nuclear Eya levels FCs along the anterior-posterior axis Each data point represents a single cell.								
	Stage 5	Stage 6	Stage 7	Stage 8	Stage 9	Stage 10a	Stage 10a	Stage 10b	Stage 11
N	4	3	3	3	3	3	3	3	3
Regression	Linear	Linear	LOESS	LOESS	LOESS	LOESS	LOESS	LOESS	LOESS

Figure S2f			
Statistical Analysis	Descriptive Statistics and local polynomial regression fitting (LOESS)		
Data	Genotype: w^{1118} Nuclear Eya levels in anterior and mid+posterior FC populations. Each intensity value corresponds to the mean of a FC population of one egg chamber. To determine FC population mean intensities at least 10 nuclei were quantified.		
LOESS	Anterior population Degree of polynomial: 2 Level of CI: 0.95 Size of neighbourhood for fitting: 0.5	Mid + posterior population Degree of polynomial: 2 Level of CI: 0.95 Size of neighbourhood for fitting: 0.5	
N	66 egg chambers		
	Phase 1:	Phase 2	Phase 3
N	27	28	11
Descriptive Statistics Descriptive Statistics	anterior population		
	Min: 45.88 Max: 110.2 Mean: 76.09 SD: 18.58 CV: 0.24	Min: 43.44 Max: 109.5 Mean: 73.91 SD: 18.47 CV: 0.25	Min: 106.9 Max: 181.0 Mean: 137.4 SD: 21.93 CV: 0.16
	posterior population		
	Min: 44.95 Max: 101.3 Mean: 72.24 SD: 17.44 CV: 0.24	Min: 11.1 Max: 53.8 Mean: 26.39 SD: 11.41 CV: 0.43	Min: 11.51 Max: 21..49 Mean: 16.41 SD: 3.266 CV: 0.20

Figure S2f									
Statistical Analysis	RM two-way Anova with Šídák's multiple comparisons test								
Data	Genotype: w^{1118} Nuclear Eya levels in anterior and mid+posterior FC populations. Each intensity value corresponds to the mean of a FC population of one egg chamber. To determine FC population mean intensities at least 10 nuclei were quantified.								
N	Stage 4	Stage 5	Stage 6	Stage 7	Stage 8	Stage 9	Stage 10a	Stage 10b	Stage 11
Anterior population	7	5	5	5	4	17	5	5	5
Mid + posterior population	7	5	5	5	4	17	5	5	5
F-Statistics	Stage x intensity					F = 75.74 on 8 and 49 DF, $p < 0.001$			
	Stage					F = 12.27 on 8 and 49 DF, $p < 0.001$			
	intensity					F = 693.4 on 8 and 49 DF, $p < 0.001$			

	Egg chamber				F = 3.44 on 8 and 49 DF, p < 0.001				
Descriptive Statistics	Stage 4	Stage 5	Stage 6	Stage 7	Stage 8	Stage 9	Stage 10a	Stage 10b	Stage 11
	Anterior population								
Mean	89.1	89.2	67.8	69.6	66.2	70.2	103	141.5	139.5
SD	14.1	22.5	18.3	6.6	17.3	16.4	6	26.2	16.1
	Mid + posterior population								
Mean	86.4	84.3	64.9	48.6	35.7	23.4	15.4	17.2	15.6
SD	12.2	18.7	16.2	7.1	9.6	7.9	1.1	3.8	3.3
Multiple Comparison	Stage 4	Stage 5	Stage 6	Stage 7	Stage 8	Stage 9	Stage 10a	Stage 10b	Stage 11
t	0.5373	0.8264	0.5	3.564	4.645	14.69	14.9	21.17	21.1
DF	49								
P	> 0.99	> 0.99	> 0.99	0.007	< 0.001	< 0.001	< 0.001	< 0.001	< 0.001

Figure 3b		
Statistical Analysis	Descriptive Statistics and two-tailed Welch's t-test	
Data	Genotype: *hsflp;; act>>UAS-ubdGFP/UAS-eya* Phase 2 egg chambers with clonal ectopic *eya* expression. Cells grouped into MBFCs ectopically expressing *eya* (eya$^+$) and control MBFCs (control). Apical surface areas were measured.	
N	3 egg chambers of similar germline size with several eya$^+$ clones	
	control: 71	*eya*$^+$: 64
Descriptive Statistics	Mean: 56.87 SD: 18.71	Mean: 117.7 SD: 45.36
Two-tailed Welch's t-test	t = 11.6 with 113.1 DF, p< 0.001	
Figure 3e		
Statistical Analysis	Descriptive Statistics and two-tailed Welch's t-test	
Data	Genotype: *hsflp; UAS-eyaRNAi; act>>Gal4, UAS-rfp* Apical surface areas of control AFCs and AFCs expressing *eyaRNA*i during Phase 2 (stage 9).	
N	3 egg chambers of similar germline size with several *eyaRNAi* expressing clones	
	control: 20	*eyaRNAi:* 20
Descriptive Statistics	Mean: 287 SD: 133.7	Mean: 64.73 SD: 21.74
Two-tailed Welch's t-test	t = 7.339 with 20 D, p < 0.001	
Figure 3h		
Statistical Analysis	Descriptive Statistics and unpaired Student's t-test	
Data	Genotype: *hsflp;; act>>UAS-ubdGFP/UAS-eya* Phase 2 egg chambers with clonal ectopic *eya* expression. Cells grouped into MBFCs ectopically expressing *eya* (eya$^+$) and control MBFCs (control). Apical surface areas were measured.	
N	3 egg chambers of similar germline size with several eya$^+$ clones	
	control: 75	*eya*$^+$: 83
Descriptive Statistics	Mean: 26.1 SD: 6.5	Mean: 27.5 SD: 8.1
Unpaired t-test	t = 1.166 with 156 DF, p=0.245	
Figure 3m		
Statistical Analysis	Welch one-way Anova with Dunnett's T3 Multiple Comparisons	
Data	Genotype: *hsflp;; act>>UAS-ubdGFP/UAS-eya* Ratio of apical vs lateral section areas in unaffected MBFCs (control), MBFCs ectopically expressing eya and in contact with eya$^-$ cells (eya$^+$) and MBFCs in direct contact with eya expressing MBFCs (neighbors).	
N	FCs of 4 different egg chambers. Control MBFCs: 16 eya$^+$ MBFCs : 14 neighbours: 18	
W	W=61.24 on 2 and 20.52 DF, p < 0.001	
Multiple Comparison	Control MBFC vs eya$^+$ MBFC: t=7.936 with 24.15 DF, p < 0.001 Control MBFC vs neighbour: t=2.812 with 23.74 DF, p=0.02	
Figure 3r		
Statistical Analysis	Descriptive Statistics and Unpaired Student's t-test	
Data	Genotype: w^{1115} Angle between anterior lateral surface and germline surface of AFC and MBFC during Phase 2 (stage 9). Angles of cells of 4 egg chambers were measured.	
N	AFC: 45	MBFC: 82
Descriptive Statistics	AFC: Mean: 38.88 SD: 14.71	MBFC: Mean: 90.05 SD: 16.15
Two-tailed t-test	t = 17.61 with 125 DF, p < 0.001	

Figure S3d		
Statistical Analysis	Two-tailed unpaired Student's t-test	
Data	Genotypes: *tj>cd8tom* & *tj>cd8tom,eyaRNAi* Ratio of perimeter shared with somatic cells (cd8-tom) vs area for individual germline cysts	
N	*tj>cd8tom* : 2 testis, 9 cysts *tj>cd8tom,eyaRNAi:* 5 testis, 10 cysts Only cysts of sizes >1000µm^2 and <1500µm^2 were used to determine perimeter/area ratios	
Descriptive statistics	*tj>cd8tom*: mean = 0.1889, SE = 0.0072	*tj>cd8tom,eyaRNAi:* mean = 0.1173, SE = 0.00363
Two-tailed unpaired t-test	Two-tailed, t = 9.165 with 17 DF, p < 0.001	
Figure S3g		
Statistical Analysis	Linear Regression	
Data	Genotype: *tj>cd8tom,ubdABD-gfp* Eya Levels (a.u.) and apical surface areas (µm^2) of FCs from anterior rows 1-7 of stage 9 egg chambers with similar germline sizes.	
N	57 FCs, 3 egg chambers	
Linear Regression	y= 17+2.7*x (y=apical surface area, x=Eya levels) R^2=0.67	

Figure 4c	
Statistical Analysis	Descriptive Statistics
Data	Genotype: w^{1118} Mean Eya fluorescence intensities of first 7 anterior rows of egg chambers from stage 5-10b. Eya row intensities as a function of time. Time derived from reported stage durations [12,13] Eya mean intensities of stages were assigned to the midpoint of each stage. Assigned relative affinities are shown.
N	stage 5: 5, stage 6: 5 , stage 7: 5 , stage 8: 4 , stage 9e: 8 , stage 9m: 9 , stage 10a: 5 , stage 10b: 5
Polynomial Regression	For each row dynamic a least squares approximation by sixth-order polynomial constrained to have vanishing derivative at t = 0 and t = 36 hours was generated. See table S7 for coefficients.
Figure 4e	
Statistical Analysis	Descriptive Statistics
Data	genotype: *tj>cd8tom,ubdABD-gfp* Apical surface areas of first 7 anterior rows for stage 7,8,9e,9m & 10 (pooled stage 10a and 10b) egg chambers
N	Stage 7: 4, stage 8: 3, stage 9e: 5, stage 9m: 5, stage 10: 3
LOESS	Discrete independent variable, therefore LOESS fitted curve just for visualization of gradient development.
Figure 4f	
Statistical Analysis	Descriptive Statistics
Data	Apical length measurements of the results of the phase field model describing the collective behaviour of FCs as a function of their affinity. Apical length were measured and squared to generate approximations of apical surface areas of the first 7 anterior rows for stage 7-10a.
LOESS	Discrete independent variable, therefore LOESS fitted curve just for visualization of gradient development.

Figure S4f		
Statistical Analysis	Linear Regression	
Data	Genotype: *hsflp;; act>>UAS-ubdGFP/UAS-eya* Apical surface areas of control AFCs and eya^{OE} AFCs as a function of their distance to the anterior tip. Data of each egg chamber were normalized for the distance and the apical surface area.	
N	control FCs: 71 FC, 3 EC	eya^{OE} FCs: 65 FC, 3 EC
Linear regression	Apical surface area ~ distance to anterior tip	
	F-statistic: 160.4 on 1 and 69 DF, $p < 0.001$, Adj. R^2=0.69	F-statistic: 0.4947 on 1 and 63 DF, $p = 0.48$, Adj. R^2=-0.0008

Figure 5f				
Statistical Analysis	Local polynomial regression fitting (LOESS)			
Data	Genotypes: *mirr>gfp & mirr>eya* Egg chambers manually selected to sufficiently cover egg chamber development from stage 2 to 12. Therefore, frequencies are not representative of population frequencies.			
N	*mirr>gfp*: 153		*mirr>eya*: 157	
LOESS	*mirr>gfp*		*mirr>eya*	
OCC proportion	Degree of polynomial: 2 Level of CI: 0.95 Size of neighbourhood for fitting: 0.5		Degree of polynomial: 2 Level of CI: 0.95 Size of neighbourhood for fitting: 0.5	
Statistical Analysis	Multiple Linear Regression with Interaction Y ~ germline size + genotype + germline size * genotype If $p \geq 0.05$ for the interaction effect: multiple linear regression without interaction Y ~ germline size + genotype			
Data	Genotypes: *mirr>gfp* & *mirr>eya* Subset 1: 5000 μm^2 < germline size > 11650 μm^2 Subset 2: 11650 μm^2 < germline size > 31500 μm^2			
N	subset 1 *mirr>gfp*: 26	subset 1 *mirr>eya*: 31	subset 2 *mirr>gfp*: 41	Subset 2 *mirr>eya*: 44
Multiple Linear Regression	Y ~ germline size + genotype + germline size * genotype		Y ~ germline size + genotype	
OCC proportion	Subset1 F-statistic: 15.96 on 3 and 53 DF, $p < 0.001$, Adj. R^2=0.445 Genotype*Germline Size p = 0.206		Subset1 F-statistic: 22.84 on 2 and 54 DF, $p < 0.001$, Adj. R^2=0.438 Genotype effect: 0.025, p =0.028	
	Subset2 F-statistic: 53.71 on 3 and 81 DF, $p < 0.001$, Adj. R^2=0.653 Genotype*Germline Size $p < 0.001$			

Figure S5b					
Statistical Analysis	Descriptive Statistics				
Data	Genotype: *mirr>gfp* Cell count of posterior FCs without GFP in 2D-crosssections and its proportion of all FCs				
N	80 egg chambers				
Descriptive Statistics	Posterior GFP^- cells				
	Min = 14	Max = 27	Mean = 21.23	SD = 2.47	CV = 0.116
	Proportion of posterior GFP^- cells				
	Min = 0.206	Max = 0.4138	Mean = 0.3305	SD: 0.041	CV = 0.124
Figure S5c					
Statistical Analysis	Local polynomial regression fitting (LOESS)				
Data	Genotype: *mirr>gfp* and *mirr>eya* Total cell count of egg chambers of all phases.				
N	*mirr>gfp*: 153		*mirr>eya*: 157		
Local polynomial regression fitting parameters	Degree of polynomial: 2 Level of CI: 0.95 Size of neighbourhood for fitting: 0.5		Degree of polynomial: 2 Level of CI: 0.95 Size of neighbourhood for fitting: 0.5		
Statistical Analysis	Descriptive statistics and two-tailed Student's t-test				
Data	Total cell count of *mirr>gfp* and *mirr>eya* in all egg chambers with germline sizes > 6500 μm^2 and < 29000 μm^2 (Phase 2).				

N	mirr>gfp: 57		mirr>eya: 67	
Descriptive Statistics	Mean = 65 SD= 3.24		Mean = 60 SD = 3.93	
Two-tailed unpaired t-test	t = 7.97 with 122 DF, p < 0.001			
Figure S5d				
Statistical Analysis	Two intersection lines – fit the crossing point Y = Ycross + (X-Xcross)*Slope			
Data	Genotype: mirr>gfp Subset of germline sizes of > 6000 µm^2 and < 20000 µm^2 OCC proportion was used for linear regression of FC displacement. Proportion of posterior FC without GFP of each egg chamber with GFP signal was used to interpolate the proportion of posterior FCs without GFP.			
N	OCC proportion: 41 egg chambers		PFCs without GFP: 36 egg chambers	
Fit of crossing point	Ycross		Xcross	
Best-fit values	0.3161		11653	
95% CI	0.3032 – 0.3279		10632 - 12569	
Goodness of Fit	73 DF, R^2 = 0.6377			
Figure S5e				
Statistical Analysis	Two-Way Anova with Šídák's multiple comparisons test			
Data	Genotypes: *mirr>gfp* & *mirr>eya* Only egg chambers with germline sizes < 40000 µm^2 (as mirr>eya egg chambers do not become bigger) Subset 1: germline size < 11650 µm^2 Subset 2: germline size > 11650 µm^2			
N	*mirr>gfp* <11650µm^2 74	*mirr>eya* <11650µm^2 86	*mirr>gfp* >11650µm^2 74	*mirr>eya* >11650µm^2 71
Two-Way Anova				
OCC proportion	Interaction: 101.3 on 1 and 301 DF, p < 0.001 Germline size: 534.9 on 1 and 301 DF, p < 0.001 Genotype: 79.39 on 1 and 301 DF, p < 0.001			
Multiple Comparison	*mirr>gfp* <11650µm^2 vs. *mirr>eya* <11650µm^2		*mirr>gfp* >11650µm^2 vs. *mirr>eya* >11650µm^2	
OCC proportion	t = 0.8357 with 301 DF, p = 0.64		t = 13.11 with 301 DF, p < 0.001	

	Figure 6 c,h,i		
Statistical Analysis	Local polynomial regression fitting (LOESS), descriptive statistics and linear regression with y ~ germline size		
Data	Genotype: *wt* (w^{1118}) Multidimensional egg chamber morphology dataset. Parameters plotted against germline size.		
N	126 egg chambers manually selected to sufficiently cover egg chamber development from stage 2 to 12. Frequencies are not representative of population stage or size frequencies. Phase 1: 62, Phase 2: 39, Phase 3: 26		
Descriptive Statistics	**c)** Interface Angle	**h)** OO-FC interface proportion	**i)** OO area proportion
LOESS	Degree of polynomial: 2 Level of CI: 0.95 Size of neighbourhood for fitting: 0.4	Degree of polynomial: 2 Level of CI: 0.95 Size of neighbourhood for fitting: 0.4	Degree of polynomial: 2 Level of CI: 0.95 Size of neighbourhood for fitting: 0.4
Phase 1	Min: 64.79 Max: 127.7 Mean: 99.27 SD: 15.34 CV: 0.15	Min: 0.079 Max: 0.184 Mean: 0.132 SD: 0.023 CV: 0.17	Min: 0.055 Max: 0.158 Mean: 0.086 SD: 0.019 CV: 0.22
Phase 2	Min: 31.44 Max: 156.1 Mean: 60.15 SD: 25.88 CV: 0.43	Min: 0.144 Max: 0.409 Mean: 0.292 SD: 0.073 CV: 0.25	Min: 0.067 Max: 0.376 Mean: 0.19 SD: 0.082 CV: 0.43
Phase 3	Min: 134.9 Max: 180 Mean: 166.6 SD: 14.49 CV: 0.087	Min: 0.378 Max: 0.746 Mean: 0.501 SD: 0.118 CV: 0.24	Min: 0.321 Max: 0.921 Mean: 0.56 SD: 0.204 CV: 0.36
Linear Regression	Phase 1 Slope: $-8.1*10^{-4}$ Phase 2 Slope: $2.32*10^{-3}$ Phase 3 Slope: $8.23*10^{-4}$	Phase 1 Slope: $4.4*10^{-6}$ Phase 2 Slope: $1.1*10^{-5}$ Phase 3 Slope: $8.0*10^{-6}$	Phase 1 Slope: $-3.17*10^{-6}$ Phase 2 Slope: $1.22*10^{-5}$ Phase 3 Slope: $1.41*10^{-5}$

Figure 6d			
Statistical Analysis	Descriptive statistics		
Data	Genotype: *wt* (w^{1118}) Interface Angle (°)		
N	116 EC, manually selected to cover stages 2 to 11 Phase 1: 62 egg chamber, phase 2: 39 egg chamber, phase 3: 15 egg chamber		
Descriptive Statistics	Phase 1	Phase 2	Phase 3
	Median: 100 Mean: 99 SE: 2 95% CI: 95 - 103	Median: 52 Mean: 60 SE: 4 95% CI: 52 – 69	Median: 161 Mean: 156 SE: 3 95% CI: 151 – 163

Figure 6e	
Statistical Analysis	Local polynomial regression fitting (LOESS)
Data	Genotype: *wt* (w^{1118}) Eya Levels (a.u.) of FCs at the nurse cell-oocyte boundary and the corresponding interface angle.
N	54 EC, manually selected to cover stages 2 to 10b. Phase 1: 21 egg chamber, phase 2: 29 egg chamber, phase 3: 4 egg chamber
LOESS	Degree of polynomial: 2, Level of CI: 0.95, Size of neighbourhood for fitting: 0.7

Figure 6f			
Statistical Analysis	Linear Regression		
Data	Genotype: *wt (w^{1118})* Eya Levels of FCs at the nurse cell-oocyte boundary and the corresponding interface angle.		
N	36 EC, manually selected covering stage 2 to 9.		
Linear Regression	y= 44+0.64*x (y=interface angle, x=Eya levels) R^2=0.54		
Estimation of Eya Level giving rise to 90° Interface Angle	x=71.57 a.u., 95% CI: 62.7 – 83.7 a.u.		
Figure 6g			
Statistical Analysis	Descriptive statistics		
Data	Genotype: *wt (w^{1118})* Eya Levels (a.u.) of FCs at the nurse cell-oocyte boundary.		
N	52 EC, manually selected to cover stages 3 to 10b. Phase 1: 19 egg chamber, phase 2: 29 egg chamber, phase 3: 4 egg chamber		
Descriptive Statistics	Phase 1	Phase 2	Phase 3
	Median: 76 Mean: 77 SE: 4. 95% CI: 68-86	Median: 30 Mean: 42 SE: 5.7 95% CI: 31 – 54	Median: 146 Mean: 143 SE: 10 95% CI: 111 – 175
Figure 6j			
Statistical Analysis	Descriptive Statistics		
Data	Genotype: *w^{1118}* Mean Eya fluorescence intensities of first 7 anterior rows of egg chambers from stage 5-10b. Eya row intensities as a function of time. Time derived from reported stage durations [12,13]. Eya mean intensities of stages were assigned to the midpoint of each stage. Assigned effective affinities are shown.		
N	stage 5: 5, stage 6: 5 , stage 7: 5 , stage 8: 4 , stage 9e: 8 , stage 9m: 9 , stage 10a: 5 , stage 10b: 5		
Polynomial Regression	For each row dynamic a least squares approximation by sixth-order polynomial constrained to have vanishing derivative at t = 0 and t = 36 hours was generated. See table S7 for coefficients.		
Figure 6k			
Statistical Analysis	Descriptive Statistics		
Data	Genotype: *w^{1118}* Mean proportional distance from anterior tip of first 7 anterior rows of egg chambers from stage 5-10b. Mean proportional distance as a function of time. Time derived from reported stage durations [12,13]. Mean proportional distance of stages were assigned to the midpoint of each stage.		
N	stage 5: 5, stage 6: 5 , stage 7: 5 , stage 8: 4 , stage 9e: 8 , stage 9m: 9 , stage 10a: 5 , stage 10b: 5		
Polynomial Regression	For each row dynamic a least squares approximation by fifth-order polynomial constrained to have vanishing derivative at t = 0 and t = 36 hours was generated. See table S8 for coefficients.		
Figure 6m			
Statistical Analysis	Descriptive Statistics		
Data	Simulations based on wt Eya levels Measured interface angle of simulated images as a function of reported stage durations [12,13].		
LOESS	LOESS fitted curve to represent dynamics		

Figure 6n	
Statistical Analysis	Descriptive Statistics
Data	Simulations based on wt Eya levels Measured OO-FC interface proportion of simulated images as a function of reported stage durations [12,13].
LOESS	LOESS fitted curve to represent dynamics
Figure 6o	
Statistical Analysis	Descriptive Statistics
Data	Simulations based on wt Eya levels Measured proportional oocyte area of simulated images as a function of reported stage durations [12,13].
LOESS	LOESS fitted curve to represent dynamics

Figure 7b			
Statistical Analysis		Descriptive Statistics	
Data		Simulations with ectopic effective oocyte affinity from stage 5 onwards. Measured interface angle of simulated images as a function of reported stage durations [12,13].	
LOESS		LOESS fitted curve to represent dynamics	
Figure 7c			
Statistical Analysis		Descriptive Statistics	
Data		Simulations with ectopic effective oocyte affinity from stage 5 onwards. Measured OO-FC interface proportion of simulated images as a function of reported stage durations [12,13].	
LOESS		LOESS fitted curve to represent dynamics	
Figure 7d			
Statistical Analysis		Descriptive Statistics	
Data		Simulations with ectopic effective oocyte affinity from stage 5 onwards. Measured proportional oocyte area of simulated images as a function of reported stage durations [12,13].	
LOESS		LOESS fitted curve to represent dynamics	
Figure 7 g,k,l			
Statistical Analysis		Local polynomial regression fitting (LOESS)	
Data		Genotypes: *gr1>gfp & gr1>eyaRNAi* Egg chambers manually selected to sufficiently cover Phase 1 egg chamber development. Frequencies are not representative of population stage or size frequencies.	
N		*gr1>gfp*: 42	*gr1>eyaRNAi*: 60
LOESS		*gr1>gfp*	*gr1>eyaRNAi*
g	**Interface Angle**	Degree of polynomial: 2 Level of CI: 0.95 Size of neighbourhood for fitting: 0.7	Degree of polynomial: 2 Level of CI: 0.95 Size of neighbourhood for fitting: 0.7
k	**OO-FC interface**	Degree of polynomial: 2 Level of CI: 0.95 Size of neighbourhood for fitting: 0.7	Degree of polynomial: 2 Level of CI: 0.95 Size of neighbourhood for fitting: 0.7
l	**OO proportion**	Degree of polynomial: 2 Level of CI: 0.95 Size of neighbourhood for fitting: 0.7	Degree of polynomial: 2 Level of CI: 0.95 Size of neighbourhood for fitting: 0.7
Statistical Analysis		Multiple Linear Regression with Interaction Y ~ germline size + genotype + germline size * genotype If $p \geq 0.05$ for the interaction effect: multiple linear regression without interaction Y ~ germline size + genotype	

Data		Genotypes: *gr1>gfp* & *gr1>eyaRNAi* Subset 1: 500 µm^2 < germline size < 1609 µm^2 Subset 2: 1609 µm^2 < germline size < 6500 µm^2			
N		subset 1 *gr1>gfp*: 13	subset 1 *gr1>eyaRNAi*: 17	subset 2 *gr1>gfp*: 29	subset 2 *gr1>eyaRNAi*: 43
Multiple Linear Regression		Y ~ germline size + genotype + germline size * genotype		Y ~ germline size + genotype	
g	**Interface Angle**	Subset 1 F-statistic: 3.514 on 3 and 26 DF, p = 0.029, Adj. R^2=0.0.206 Genotype*Germline Size p = 0.361		Subset 1 F-statistic: 4.863 on 2 and 27 DF, p = 0.0157, Adj. R^2=0.2104 Genotype effect: 0.019, p = 0.029	
		Subset 2 F-statistic: 19.48 on 3 and 68 DF, p < 0.001, Adj. R^2=0.4385 Genotype*Germline Size p = 0.222		Subset 2 F-statistic: 28.25 on 2 and 69 DF, p < 0.001, Adj. R^2=0.4343 Genotype effect: 0.019, p < 0.001	
k	**OO-FC interface proportion**	Subset 1 F-statistic: 8.874 on 3 and 26 DF, p < 0.001, Adj. R^2=0.4489 Genotype*Germline Size p = 0.866		Subset 1 F-statistic: 13.79 on 2 and 27 DF, p < 0.001, Adj. R^2=0.4687 Genotype effect: 0.03, p < 0.001	
		Subset 2 F-statistic: 63.09 on 3 and 68 DF, p < 0.001, Adj. R^2=0.724 Genotype*Germline Size p = 0.0364			
l	**OO area proportion**	Subset 1 F-statistic: 16.2 on 3 and 26 DF, p < 0.001, Adj. R^2=0.6113 Genotype*Germline Size p = 0.214		Subset 1 F-statistic: 22.96 on 2 and 27 DF, p < 0.001, Adj. R^2=0.6023 Genotype effect: 0.019, p <0.001	
		Subset 2 F-statistic: 37.17 on 3 and 68 DF, p < 0.001, Adj. R^2=0.4923 Genotype*Germline Size p = 0.00189			
Figure 7i					
Statistical Analysis		Two-tailed unpaired Student's t-test			
Data		Genotypes: *gr1>gfp* & *gr1>eyaRNAi* Coefficient of variation of NC-FC interface proportions of NCs within their respective egg chamber Only egg chambers with germline sizes > 2000 µm^2 and <5500 µm^2 were selected. At least 3 NCs covering all rows were used to determine the CV of individual egg chambers.			
N		*gr1>gfp* : 15 egg chambers, 71 NCs		*gr1>eyaRNAi:* 15 egg chambers, 89 NCs	
Descriptive statistics		*gr1>gfp* : mean CV = 0.1191, SE = 0.01382		*gr1>eyaRNAi:* mean CV = 0.2484, SE = 0.01957	
Two-tailed unpaired t-test		Two-tailed, t=5.397 with 28DF, p < 0.001			
Figure 7j					
Statistical Analysis		Two-tailed unpaired Welch's t-test			
Data		Genotypes: *gr1>gfp* & *gr1>eyaRNAi* Coefficient of variation of NC areas normalized to germline area Only egg chambers of with germline sizes >2000 µm^2 and <5500 µm^2 were selected. At least 3 NCs covering all rows were used to determine the CV of individual egg chambers.			
N		*gr1>gfp* : 15 egg chambers, 71 NCs		*gr1>eyaRNAi:* 15 egg chambers, 89 NCs	
Descriptive statistics		*gr1>gfp* : mean = 0.2008, SE = 0.01422		*gr1>eyaRNAi:* mean = 0.3619, SE = 0.02489	
Welch's t-test		Two-tailed, t=5.618 with 22.26 DF, p < 0.001			

Figure S7b			
Statistical Analysis	Descriptive Statistics		
Data	Genotype: *gr1 > eyaRNAi* Germline sizes of egg chambers grouped by Eya presence into Eya^{+}, sporadic Eya and no Eya.		
N	Eya present: 6	sporadic Eya: 15	no Eya: 75
Descriptive Statistics	Mean: 743 µm^2 Min: 515.8 µm^2 Max: 995.1 µm^2 95% CI: 554.3 – 933.3 µm^2	Mean: 1609 µm^2 Min: 1088 µm^2 Max: 2787 µm^2 95% CI: 1300 – 1918 µm^2	Mean: 8622 µm^2 Min: 1181 µm^2 Max: 26206 µm^2 95% CI: 7167 – 10077 µm^2

Figure S7c,d,e				
Statistical Analysis	Two-Way Anova with Šídák's multiple comparisons test			
Data	Genotypes: *gr1>gfp* & *gr1>eyaRNAi* Subset 1: germline size < 1600 µm^2 Subset 2: germline size > 1600 & <6500 µm^2			
N	*gr1>gfp*		*gr1>eyaRNAi*	
	<1600 µm^2: 13	>1600 & <6500 µm^2: 27	*<1600* µm^2: 16	*<1600* & <6500 µm^2: 36
Two-Way Anova				
Interface Angle	Interaction: 6.978 on 1 and 88 DF, p = 0.01 Germline size: 14.26 on 1 and 88 DF, p < 0.001 Genotype: 438.32 on 1 and 88 DF, p < 0.001			
OO-FC interface	Interaction: 20.49 on 1 and 88 DF, p < 0.001 Germline size: 21.76on 1 and 88 DF, p < 0.001 Genotype: 68.3 on 1 and 88 DF, p < 0.001			
OO proportion	Interaction: 13.28 on 1 and 88 DF, p < 0.001 Germline size: 0.444 on 1 and 88 DF, p = 0.51 Genotype: 41.26 on 1 and 88 DF, p < 0.001			
Multiple Comparison	*gr1>gfp vs. gr1>eyaRNAi* (<1600 µm^2)		*gr1>gfp vs. gr1>eyaRNAi* (>1600 & <6500 µm^2)	
Interface Angle	t = 2.147 with 88 DF, p = 0.07		t = 87.839 with 88 DF, p < 0.001	
OO-FC interface	t = 2.262 with 88 DF, p = 0.05		t = 11.35 with 88 DF, p < 0.001	
OO proportion	t = 1.682 with 88 DF, p = 0.18		t = 8.936 with 88 DF, p < 0.001	

Figure 8b				
Statistical Analysis		Descriptive Statistics		
Data		Simulations with ectopic effective nurse cell affinity from stage 7 onwards. Measured interface angle of simulated images as a function of reported stage durations [12,13].		
LOESS		LOESS fitted curve to represent dynamics		
Figure 8c				
Statistical Analysis		Descriptive Statistics		
Data		Simulations with ectopic effective nurse cell affinity from stage 7 onwards. Measured OO-FC interface proportion of simulated images as a function of reported stage durations [12,13].		
LOESS		LOESS fitted curve to represent dynamics		
Figure 8d				
Statistical Analysis		Descriptive Statistics		
Data		Simulations with ectopic effective nurse cell affinity from stage 7 onwards. Measured proportional oocyte area of simulated images as a function of reported stage durations [12,13].		
LOESS		LOESS fitted curve to represent dynamics		
Figure 8g,h,j				
Statistical Analysis		Local polynomial regression fitting (LOESS)		
Data		Genotypes: *mirr>gfp & mirr>eya* Egg chambers manually selected to sufficiently cover egg chamber development from stage 2 to 12. Therefore, frequencies are not representative of population frequencies.		
N		*mirr>gfp*: 153	*mirr>eya*: 157	
LOESS		*mirr>gfp*	*mirr>eya*	
g	**Interface Angle**	Degree of polynomial: 2 Level of CI: 0.95 Size of neighbourhood for fitting: 0.4	Degree of polynomial: 2 Level of CI: 0.95 Size of neighbourhood for fitting: 0.4	
h	**OO-FC interface**	Degree of polynomial: 2 Level of CI: 0.95 Size of neighbourhood for fitting: 0.3	Degree of polynomial: 2 Level of CI: 0.95 Size of neighbourhood for fitting: 0.8	
j	**OO proportion**	Degree of polynomial: 2 Level of CI: 0.95 Size of neighbourhood for fitting: 0.4	Degree of polynomial: 2 Level of CI: 0.95 Size of neighbourhood for fitting: 0.4	
Statistical Analysis		Multiple Linear Regression with Interaction Y ~ germline size + genotype + germline size * genotype If $p \geq 0.05$ for the interaction effect: multiple linear regression without interaction Y ~ germline size + genotype		
Data		Genotypes: *mirr>gfp* & *mirr>eya* Subset 1: 5000 μm^2 < germline size > 11650 μm^2 Subset 2: 11650 μm^2 < germline size > 31500 μm^2		
N		subset 1 *mirr>gfp*: 26	subset 1 *mirr>eya*: 31	subset 2 *mirr>gfp*: 41	Subset 2 *mirr>eya*: 44
Multiple Linear Regression		Y ~ germline size + genotype + germline size * genotype		Y ~ germline size + genotype	
g	**Interface Angle**	Subset1 F-statistic: 19.1 on 3 and 53 DF, $p < 0.001$, Adj. R^2=0.4923 Genotype*Germline Size $p < 0.001$			

		Subset2 F-statistic: 85.22 on 3 and 81 DF, $p < 0.001$, Adj. R^2=0.75 Genotype*Germline Size p = 0.826	Subset2 F-statistic: 129.3 on 2 and 82 DF, $p < 0.001$, Adj. R^2=0.75 Genotype effect: $p < 0.001$
h	**OO-FC interface proportion**	Subset 1 F-statistic: 8.879 on 3 and 53 DF, $p < 0.001$, Adj. R^2= 0.297 Genotype*Germline Size p = 0.054	Subset1 F-statistic: 12.93 on 2 and 54 DF, $p < 0.001$, Adj. R^2=0.2988 Genotype effect: p =0.1434
		Subset 2 F-statistic: 81.86 on 3 and 81 DF, $p < 0.001$, Adj. R^2=0.74 Genotype*Germline Size $p < 0.001$	
j	**OO area proportion**	Subset 1 F-statistic: 34.36 on 3 and 53 DF, $p < 0.001$, Adj. R^2=0.64 Genotype*Germline Size $p < 0.001$	
		Subset 2 F-statistic: 40.57 on 3 and 81 DF, $p < 0.001$, Adj. R^2=0.59 Genotype*Germline Size $p < 0.001$	

Figure 8i		
Statistical Analysis	Two-Way Anova with Šídák's multiple comparisons test	
Data	Genotypes: *mirr>gfp* & *mirr>eya* NC-FC interface proportion of NC perimeter for individual nurse cells .NC are grouped by NC row and averaged within each egg chamber. NC row averages of different egg chambers are analysed.	
N	*mirr>gfp* egg chamber: N=8 row averages: A: 8, MA: 6, MP: 8, P: 8	*mirr>eya* egg chambers: N=9 individual nurse cells: A: 7, MA: 9, MP: 9, P: 9
Descriptive Statistics	*mirr>gfp* A: mean = 0.488, SE = 0.032 MA: mean = 0.398, SE = 0.021 MP: mean = 0.306, SE = 0.01 P: mean = 0.287, SE = 0.014	*mirr>eya* A: mean = 0.416, SE = 0.048 MA: mean = 0.337, SE = 0.021 MP: mean = 0.297, SE = 0.018 P: mean = 0.406, SE = 0.014
F	Interaction: 6.828 on 3 and 56DF, $p < 0.001$ NC row: 13.86 on 3 and 56 DF, $p < 0.001$ Genotype: 0.09731 on 3 and 56 DF, p = 0.76	
Multiple Comparison	*mirr>gfp* vs *mirr>eya* for each NC row A: t= 2.062 with 56 DF, p = 0.16 MA: t= 1.701 with 56 DF, p = 0.33 MP: t= 0.2504 with 56 DF, $p > 0.99$ P: t= 3.644 with 56 DF, p = 0.002	

Figure S8a,b,c				
Statistical Analysis	Two-Way Anova with Šídák's multiple comparisons test			
Data	Genotypes: *mirr>gfp* & *mirr>eya* Only egg chambers with germline sizes < 40000 µm^2 (as mirr>eya egg chambers do not become bigger) Subset 1: germline size < 11650 µm^2 Subset 2: germline size > 11650 µm^2			
N	*mirr>gfp* <11650µm^2 74	*mirr>eya* <11650µm^2 86	*mirr>gfp* >11650µm^2 74	*mirr>eya* >11650µm^2 71
Two-Way Anova				

Interface Angle	Interaction: 3.653 on 1 and 301 DF, p = 0.06 Germline size: 30.21 on 1 and 301 DF, p < 0.001 Genotype: 47.55 on 1 and 301 DF, p < 0.001			
OO-FC interface	Interaction: 112.7 on 1 and 301 DF, p < 0.001 Germline size: 311.9 on 1 and 301 DF, p < 0.001 Genotype: 98.45 on 1 and 301 DF, p < 0.001			
OO proportion	Interaction: 27.4 on 1 and 301 DF, p < 0.001 Germline size: 189.8 on 1 and 301 DF, p < 0.001 Genotype: 10.85 on 1 and 301 DF, p = 0.001			
Multiple Comparison	*mirr>gfp* <11650µm^2 vs. *mirr>eya* <11650µm^2		*mirr>gfp* >11650µm^2 vs. *mirr>eya* >11650µm^2	
OO-FC interface	t = 0.5035 with 301 DF, p = 0.85		t = 14.2 with 301 DF, p < 0.001	
OO proportion	t = 1.412 with 301 DF, p = 0.29		t = 5.901 with 301 DF, p < 0.001	
Interface Angle	t = 3.609 with 301 DF, p < 0.001		t = 6.087 with 301 DF, p < 0.001	
Figure S8d,e,f				
Statistical Analysis	Two-Way Anova with Šídák's multiple comparisons test			
Data	Genotypes: *tj>gfp* & *tj>λtop* Subset 1: germline size >600µm^2 & <*6500*µm^2 Subset 2: germline size >*6500*µm^2 & <31500µm^2 Subset 3: germline size >*31500*µm^2 & <62000µm^2			
N	*tj>gfp* subset 1 N: 36	*tj>λtop* subset 1 N: 55	*tj>gfp* subset 2 N: 21	*tj>λtop* subset 2 N: 13
Two-Way Anova				
Interface Angle	Interaction: 35.85 on 2 and 214 DF, p < 0.001 Germline size: 225.2 on 2 and 214 DF, p < 0.001 Genotype: 62.85 on 1 and 214 DF, p < 0.001			
OO-FC interface	Interaction: 3.34 on 2 and 214 DF, p = 0.04 Germline size: 296.2 on 2 and 214 DF, p < 0.001 Genotype: 5.136 on 1 and 214 DF, p = 0.02			
OO proportion	Interaction: 7.894 on 2 and 214 DF, p < 0.001 Germline size: 262.1 on 2 and 214 DF, p < 0.001 Genotype: 11.92 on 1 and 214 DF, p < 0.001			
Multiple Comparison	Subset 1: *tj>gfp* vs. *tj>λtop*	Subset 2: *tj>gfp* vs. *tj>λtop*	Subset 3: *tj>gfp* vs. *tj>λtop*	
Interface Angle	t = 1.125 with 214 DF, p = 0.6	t = 0.005 with 214 DF, p > 0.99	t = 9.29 with 214 DF, p < 0.001	
OO-FC interface	t = 0.103 with 214 DF, p > 0.99	t = 0.0165 with 214 DF, p > 0.99	t = 2.77 with 214 DF, p = 0.02	
OO proportion	t = 0.107 with 214 DF, p > 0.99	t = 0.027 with 214 DF, p > 0.99	t = 4.26 with 214 DF, p < 0.001	

Figure 9b					
Statistical Analysis		Descriptive Statistics			
Data		Simulations with ectopic effective oocyte affinity from stage 6 onwards. Measured interface angle of simulated images as a function of reported stage durations [12,13].			
LOESS		LOESS fitted curve to represent dynamics			
Figure 9c					
Statistical Analysis		Descriptive Statistics			
Data		Simulations with ectopic effective oocyte affinity from stage 6 onwards. Measured OO-FC interface proportion of simulated images as a function of reported stage durations [12,13].			
LOESS		LOESS fitted curve to represent dynamics			
Figure 9d					
Statistical Analysis		Descriptive Statistics			
Data		Simulations with ectopic effective oocyte affinity from stage 6 onwards. Measured proportional oocyte area of simulated images as a function of reported stage durations [12,13].			
LOESS		LOESS fitted curve to represent dynamics			
Figure 9g,h,i					
Statistical Analysis		Local polynomial regression fitting (LOESS)			
Data		Genotypes: *tj>gfp* & *tj>λtop* Egg chambers manually selected to sufficiently cover egg chamber development from stage 2 to 12. Therefore, frequencies are not representative of population frequencies.			
N		*tj>gfp*: 122		*tj>λtop*: 109	
LOESS		*tj>gfp*		*tj>λtop*	
g	**Interface Angle**	Degree of polynomial: 2 Level of CI: 0.95 Size of neighbourhood for fitting: 0.3		Degree of polynomial: 2 Level of CI: 0.95 Size of neighbourhood for fitting: 0.3	
h	**OO-FC interface proportion**	Degree of polynomial: 2 Level of CI: 0.95 Size of neighbourhood for fitting: 0.3		Degree of polynomial: 2 Level of CI: 0.95 Size of neighbourhood for fitting: 0.3	
i	**OO proportion**	Degree of polynomial: 2 Level of CI: 0.95 Size of neighbourhood for fitting: 0.3		Degree of polynomial: 2 Level of CI: 0.95 Size of neighbourhood for fitting: 0.3	
Statistical Analysis		Multiple Linear Regression with Interaction Y ~ germline size + genotype + germline size * genotype If $p \geq 0.05$ for the interaction effect: multiple linear regression without interaction Y ~ germline size + genotype			
Data		Genotypes: *tj>gfp* & *tj>λtop* Subset 1: 6500 μm^2 < germline size > 31500μm^2 Subset 2: 31500 μm^2 < germline size > 62000 μm^2			
N		subset 1 *tj>gfp*: 39	subset 1 *tj>λtop*: 58	subset 2 *tj>gfp*: 18	subset 2 *tj>λtop*: 10
Multiple Linear Regression		Y ~ germline size + genotype + germline size * genotype		Y ~ germline size + genotype	
g	**Interface Angle**	Subset1 F-statistic: 0.2759 on 3 and 93 DF, p = 0.84, Adj. R^2=-0.023			
		Subset2			

		F-statistic: 36.23 on 3 and 24 DF, $p < 0.001$, Adj. R^2=0.7965 Genotype*Germline Size p = 0.017	
h	**OO-FC interface proportion**	Subset 1 F-statistic: 450.5 on 3 and 93 DF, $p < 0.001$, Adj. R^2= 0.9335 Genotype*Germline Size p = 0.0222	
		Subset 2 F-statistic: 18.82 on 3 and 30 DF, $p < 0.001$, Adj. R^2=0.6645 Genotype*Germline Size p = 0.9727	Subset 2 F-statistic: 29.41 on 2 and 25 DF, $p < 0.001$, Adj. R^2=0.678 Genotype effect: $p < 0.001$
i	**OO area proportion**	Subset 1 F-statistic: 252.8 on 3 and 93 DF, $p < 0.001$, Adj. R^2=0.887 Genotype*Germline Size $p < 0.001$	
		Subset 2 F-statistic: 27.16 on 3 and 24 DF, $p < 0.001$, Adj. R^2= 0.744 Genotype*Germline Size p = 0.478	Subset 2 F-statistic: 41.27 on 2 and 25 DF, $p < 0.001$, Adj. R^2=0.749 Genotype effect: $p < 0.001$

Supplementary References

1. Allen, S. M. & Cahn, J. W. Microscopic Theory for Antiphase Boundary Motion and Its Application to Antiphase Domain Coarsening. *Acta Metallurgica* 27, 1085–1095 (1979).
2. Nonomura, M. Study on Multicellular Systems Using a Phase Field Model. *PLoS ONE* 7, e33501 (2012).
3. Moure, A. & Gomez, H. Phase-Field Modeling of Individual and Collective Cell Migration. *Archives of Computational Methods in Engineering* 28, 311–344 (2021).
4. Wenzel, D. & Voigt, A. Multiphase field models for collective cell migration. *Phys. Rev. E* 104, 054410 (5 Nov. 2021).
5. Garcke, H., Lam, K. F. & Rocca, E. Optimal control of treatment time in a diffuse interface model of tumor growth. *Appl. Math. Optim.* 78, 495–544 (2018).
6. Fritz, M., Lima, E. A. B. F., Nikolić, V., Oden, J. T. & Wohlmuth, B. Local and nonlocal phase-field models of tumor growth and invasion due to ECM degradation. *Math. Models Methods Appl. Sci.* 29, 2433–2468 (2019).
7. Chen, L.-Q. & Yang, W. Computer simulation of the domain dynamics of a quenched system with a large number of nonconserved order parameters: The grain-growth kinetics. *Physical Review B* 50, 15752–15756 (1994).
8. Fan, D., Geng, C. & Chen, L.-Q. Computer simulation of topological evolution in 2-D grain growth using a continuum diffuse-interface field model. *Acta Materialia* 45, 1115–1126 (1997).
9. Modica, L. & Mortola, S. Un esempio di Γ−-convergenza. *Boll. Un. Mat. Ital. B (5)* 14, 285–299 (1977).
10. Ahrens, J., Geveci, B. & Law, C. Paraview: An end-user tool for large data visualization. *The visualization handbook* 717 (2005).
11. Ayachit, U. *The ParaView Guide: A Parallel Visualization Application* (Kitware, Inc., Clifton Park, NY, USA, 2015).
12. Spradling, A. C. Developmental genetics of oogenesis. *The development of Drosophila melanogaster*, 1-70 (1993).
13. Horne-Badovinac, S. & Bilder, D. Mass transit: epithelial morphogenesis in the Drosophila egg chamber. *Developmental dynamics : an official publication of the American Association of Anatomists* 232, 559-574, doi:10.1002/dvdy.20286 (2005).